The Journal of Neuroscience, July 1, 1999, *19*(13):5528–5548

Arginine Analogs Modify Signal Detection by Neurons in the Visual Cortex

Prakash Kara and Michael J. Friedlander

Department of Physiology & Biophysics and Department of Neurobiology, University of Alabama at Birmingham, Birmingham, Alabama 35294

Nitric oxide (NO) modulates neurotransmitter release, induction of long-term synaptic potentiation and depression, and activity levels of neurons. However, it is not known whether NO contributes to the ability of the CNS to distinguish sensory signals from background noise and/or extract sensory information with greater reliability. We addressed these questions in the visual cortex, *in vivo*, using electrophysiological recording and analysis of signal detection from individual neurons. This was combined with microiontophoretic application of arginine analogs that either upregulate or downregulate the brain's endogenous NO-generating pathways or compounds that produce exogenous NO. Protocols that enhance NO levels generally increased the number of action potentials per trial evoked by visual stimuli, improved signal detection, and decreased the coefficient of variation of visually evoked responses, whereas NO-reducing protocols predominantly had complementary effects. Control experiments demonstrate that these effects are likely attributable to the specific ability of these arginine compounds to modify NO levels versus other nonspecific effects. Differential effects between neighboring cells and between single-cell receptive subfields suggest that these actions have a significant direct neural component versus exclusively operating indirectly on neurons through the central vascular actions of NO.

Key words: nitric oxide; visual cortex; signal detection; arginine; nitric oxide synthase; striate cortex; information processing; signal-to-noise

Within the network of cerebral cortical neurons, synapses are a primary locus for undergoing adaptive changes (Singer, 1995; Markram and Tsodyks, 1996). Such modulation of synaptic strength may play a role in training-induced reorganization of sensory maps and an enhanced representation of salient features in the environment and thus influence behavioral plasticity (Ahissar et al., 1992; Recanzone et al., 1993; Cruikshank and Weinberger, 1996). However, the cellular signaling pathways that underlie these processes are poorly understood. The membrane-permeant signaling molecule nitric oxide (NO) has the potential for contributing to such adaptive signal processing in the cerebral cortex, because (1) the enzyme responsible for synthesizing NO in neurons, type I nitric oxide synthase (NOS), is richly distributed in the cortical synaptic neuropile (Aoki et al., 1993, 1997; Friedlander et al., 1996); (2) NOS activation is calcium- (and thus activity-) dependent (Moncada et al., 1991; Marletta, 1994; Montague et al., 1994; Nathan and Xie, 1994; Friedlander and Gancayco, 1996); (3) NO production can modulate the release of glutamate and other neurotransmitters at cortical synapses *in vitro* (Montague et al., 1994; Ohkuma et al., 1995, 1996) and *in vivo* (Strasser et al., 1994; Kano et al., 1998); and (4) cortical NMDA receptor activation contributes to NO production (Montague et al., 1994; Kano et al., 1998). Moreover, NO has been shown to play a role in synaptic plasticity in other brain regions, e.g., NMDA receptor-dependent CA1 hippocampal long-term synaptic potentiation (LTP; Schuman and Madison, 1991, 1994; Arancio et al., 1996; Son et al., 1996; Malen and Chapman, 1997) and NMDA receptor-independent cerebellar long-term synaptic depression (LTD; Shibuki and Okada, 1991; Lev-Ram et al., 1997). Thus, the production, local diffusion, and action of NO appear to be linked to an associative, activity-dependent modulation of synaptic strength. We propose that NO could contribute to a selective amplification of groups of synapses in volumes of sensory cortex effectively increasing signal detection by individual cortical neurons. To evaluate this hypothesis, it is necessary to study the effects of NO *in vivo* in a setting that allows activiation of cortical networks by presentation of stimuli through the natural receptor apparatus versus relying exclusively on simultaneous and temporally punctate electrical stimulation of groups of cortical afferents as delivered *in vitro*.

Although NO is implicated in synaptic plasticity in other brain regions (e.g., LTP in hippocampus and LTD in cerebellum), regional inhibition of visual cortex NOS activity *in vivo* during early postnatal development does not prevent the ocular dominance shift produced by monocular visual deprivation (Reid et al., 1996; Ruthazer et al., 1996). However, other *in vivo* studies have shown that the activity levels and responsiveness of thalamic (Do et al., 1994; Cudeiro et al., 1996) and cortical (Cudeiro et al., 1997) neurons can be modified by NOS inhibition. But an explicit role for endogenous cortical NO in cortical information processing has not been explored. For example, it is not known whether the biochemical actions described for NO *in vitro* or its ability to modify firing levels of central neurons *in vivo* play a role in detection of sensory signals and/or enabling neurons to process

Received Jan. 14, 1999; revised April 20, 1999; accepted April 22, 1999.

This work was funded by National Institutes of Health Grant EY 05116 and the Helen Keller Eye Research Foundation. The following individuals provided useful discussions for this study: Trevor W. Stone (iontophoresis methods and controls), Daniel Shultz (multielectrode fabrication), Michael N. Shadlen (measurement of variability in cortex), and Joseph S. Beckman (NO chemistry). Izumi Ohzawa, Tim J. Gawne, Michael W. Quick, and Laura Schrader provided helpful comments on earlier versions of this manuscript. Felicia Hester and Vetria Byrd provided technical support. La Verne Croom provided word-processing support.

Correspondence should be addressed to Michael J. Friedlander, Department of Neurobiology, University of Alabama at Birmingham, CIRC 516, 1719 Sixth Avenue, South, Birmingham, AL 35294.

Dr. Kara's present address: Department of Neurobiology, Harvard Medical School, Boston, MA, 02115.

information with greater reliability. Nor have the specificity of the actions of NO on neighboring neurons and its potentially more subtle effects on the organization of sensory neuron spatial response profiles been explored *in vivo*.

In the present study, an *in vivo* cat visual cortex preparation was used to address four major questions: (1) Can local microiontophoretic application of compounds that are known to modify NO levels alter the visual responsiveness of individual neurons in a predictable way? (2) What are the nature, persistence, and uniformity of these effects of NO-mediating compounds between cells? (3) Are these effects attributable to NO (or its downstream reactions) or to other nonspecific actions of the iontophoresis procedures? (4) Can these same compounds that modify NO production specifically affect signal detection and/or the trial-by-trial visual response regularity of cortical neurons? These four questions were addressed, respectively, by evaluating for individual neurons the effects of (1) iontophoresis of the endogenous NOS substrate L-arginine (L-ARG), an exogenous NO generator [diethylamine NONOate (DEA-NO)], or the endogenous NOS inhibitors L-nitro-arginine (L-NA) or L-mono-methyl arginine (L-MMA); (2) these same compounds on visual responses and receptive field subfield structural organization before, during, and after their iontophoretic application and on simultaneously recorded neighboring neurons; (3) inactive forms including equivalent D-isoforms of these same compounds and application of other related L-amino acids; and (4) trial-by-trial analysis of single-cell visual responses as evaluated by calculating neuronal receiver operating characteristic (ROC) curves and coefficient of variation (CV) analysis.

Application of compounds to enhance endogenous NO production or produce exogenous NO primarily enhanced visual responses of individual neurons, although in some cases the responses were reduced. These effects were specific to the active forms of the endogenous and exogenous NO-modulating compounds and were consistent with their effects being caused by NO per se. A particularly striking effect of L-ARG was its capacity to improve signal detection and reduce the coefficient of variation of visual responses for some neurons, whereas NOS inhibitors had complementary effects. Although the sites of action of NO cannot be definitively ascertained in an *in vivo* study, our results are consistent with a specific neuronal effect of the NO-modifying compounds. Based on our findings that modulation of NO can differentially affect the visual responses of simultaneously recorded neighboring neurons and the spatial profiles of their receptive subfields, we hypothesize that endogenous cortical NO can act directly on neuronal and synaptic targets (vs acting exclusively indirectly through the vasculature). This hypothesis is consistent with observations of the direct neuronal effects of NO observed *in vitro*.

MATERIALS AND METHODS

Preparation and anesthesia. Experiments were performed on 36 anesthetized and paralyzed cats (20 kittens, 4–8 weeks old; and 16 adults cats, >6 months of age). Surgical anesthesia was induced with 3% vaporized halothane in a 1:1 mixture of N_2O/O_2. After surgical anesthesia was effected, as ascertained by the absence of corneal and footpad withdrawal reflexes, the halothane level was reduced and maintained at 2.0–2.5%, as needed. Continuous intra-arterial heart rate and blood pressure were monitored throughout the remaining surgical and subsequent electrophysiological recordings. Mean systemic blood pressure was kept between 90 and 110 mmHg. During electrophysiological recording, anesthesia was maintained with 2–3 $mg \cdot kg^{-1} \cdot hr^{-1}$ intravenous alphaxalone and alphadolone acetate (Saffan; Pitman-Moore, Washington Crossing, NJ). Further analgesia was provided with a 70:30 mixture of N_2O and O_2. Paralysis was maintained with 12 $mg \cdot kg^{-1} \cdot hr^{-1}$ gallamine triethiodide (Sherwood-Davis and Geck, St. Louis, MO) and 0.25 $mg \cdot kg^{-1} \cdot hr^{-1}$ tubocurarine chloride (Eli Lilly, Indianapolis, IN). All anesthetic and paralytic solutions were prepared in 5% dextrose and lactated Ringer's solution (Abbott Laboratories, Chicago, IL) and delivered at a rate of 3–5 ml/hr via an infusion pump. Pressure points and incision sites were treated with a topical anesthetic (Lidocaine HCl 2% jelly, Copley, Canton, MA). Animals were mechanically ventilated, and expired CO_2 was regulated at 3.8–4.2%. Body temperature was kept at 38.0°C with a feedback blanket. Pupils were dilated with 1% ophthalmic atropine sulfate (Bausch & Lomb, Rochester, NY), and the corneas were protected with neutral gas-permeable hard contact lenses (Abba Optical). A fiber optic light source was used to reflect various retinal landmarks onto a tangent screen placed 57 cm in front of the eyes (Pettigrew et al., 1979). This enabled the easy viewing and plotting of the optic disks, area centrali, and retinal blood vessels. Adequate optical refraction was obtained by focusing surface retinal blood vessels using + or − spherical lenses, which were placed in front of the eyes. In some animals, the above method of corrective refraction was complemented with streak retinoscopy. In a few cases, the positions of the area centrali before and after pharmacological manipulations (see below) were measured to ensure that changes in the evoked neuronal responses were not a result of drift of the eye position.

All single- and dual-unit electrophysiological records were obtained from the medial bank of the striate visual cortex (area 17) using platinum-plated tungsten-in-glass electrodes (Merrill and Ainsworth, 1972). Five-barrel glass micropipettes were attached to the recording electrode to iontophoretically administer (Neuro Phore BH-2; Medical Systems, Greenvale, NY) pharmacological agents in the vicinity of the recording site. The tungsten recording electrode protruded the multibarrel micropipettes by 30–50 μm. The total tip diameter of all five drug barrels together was kept between 4 and 5 μm, resulting in a tip diameter for each of the five barrels of ~1 μm.

Visual stimulation, classification of striate cortical neurons, and protocol. All visual stimuli were generated on a Tektronix (Wilsonville, OR) 608 monitor and controlled by a Picasso CRT image generator (Innisfree Ltd.). Visual stimuli were always presented monocularly and typically comprised light or dark bars and edges. Background luminance on the monitor was kept constant at 14.8 cd/m^2. The intensity of light and dark stimuli were 31 and 7.2 cd/m^2, respectively. These intensities provided Rayleigh–Michelson contrasts close to 35% for both light and dark stimuli. Light and dark drifting edges presented in random order were used to assess the receptive field structure (e.g., simple vs complex) of individual cortical cells recorded from the striate cortex (area 17). Bars of light (0.3–0.5° wide and 1.0–5.0° long) drifting across the receptive field were used before, during, and after pharmacological manipulations of the nitric oxide generating system. Interstimulus intervals were usually of times equal to the duration of the stimulus presentation. For the purposes of evaluating the contribution of NO to recorded visual responses, stimuli were presented at the orientation and direction optimal to the recorded single unit. Typically, 30–60 stimulus repetitions were used before, during, and after iontophoretic application of the various compounds. For any particular cell, the identical number of stimulus presentations was used for the different conditions.

Data collection. Continuous capture of amplified neuronal discharge signals (20 kHz), blood pressure (0.5 kHz), cortical blood flow (0.5 kHz), stimulus duration (1 kHz), and stimulus triggers (1 KHz) were processed by a real-time intelligent interface (CED 1401 Plus; Cambridge Electronic Design, Cambridge, UK) and dumped via a PCI bus to the hard drive of a personal computer equipped with a 200 MHz Pentium Pro central processing unit (Micron Electronics, Nampa, ID) with 64 MB RAM and 4 MB VRAM graphics controller (Number Nine, Lexington, MA). This processing capability together with Spike 2 for Windows (Cambridge Electronic Design) software allowed for near-real-time, trial-by-trial updates of the visual response plotted as peristimulus time histograms, raster plots, spike counts, peak firing frequencies, and interspike interval histograms. One or two units recorded from the same recording electrode were discriminated using either a Spike 2 waveform template-matching algorithm or windowed amplitude discrimination (customized script in Spike 2 software). Statistical analyses of discriminated neuronal discharge data were performed off-line. In some experiments ($n = 5$), cerebral blood flow (CBF) was measured with a 480-μm-diameter needle probe attached to a dual-channel laser Doppler flow (LDF) meter (Micro Flo DSP; Optronix Ltd., Oxford, UK). The infrared laser light (780 nm) emitter and back-scatter receiver were housed within

a single probe. The exposed tip of the probe was placed on the surface of the visual cortex away from large surface vessels to avoid response saturation. The LDF method provides continuous measurement of blood cell perfusion in the microvasculature by producing an output signal that is proportional to the blood cell flux. The LDF displays blood flow as arbitrary blood perfusion units allowing for relative *in vivo* measures of CBF (Obeid et al., 1990). Using this method, cerebral blood flow was measured either during microiontophoresis of NO-modulating compounds or in response to a hypercapnia-induced global increase in CBF by inhalation of 5% CO_2 (Irikura et al., 1995; Fabricius et al., 1996), concomitant with electrophysiological recording from individual visual cortical neurons.

Data analysis of neuronal discharges after pharmacological manipulations. For each tested neuron, under each condition (control, drug, and recovery), trial-by-trial spike counts during visual stimulation were plotted for control, drug, and recovery conditions. Significance of effects with individual drugs was confirmed by Mann–Whitney and Kruskal–Wallis tests. The minimum significance level was set at $p < 0.05$ for mean spike count comparisons.

In addition to the mean spike count tests, ROC curves were plotted for each cell before and during various pharmacological manipulations. The ROC method provides a distribution-free measure of the ability of the neuron to discriminate signal (visual activity) from noise (background activity) (Macmillan and Creelman, 1991; Guido et al., 1995). ROC curves were constructed by plotting the cumulative probability distributions of spike counts in two equivalent-sized windows. The first window was taken during the idle time (no visual stimulus present) and thus referred to as noise. The second window was taken during presentation of the visual stimulus and thus referred to as signal. The sizes of these windows were always identical (for a given cell) under control and drug conditions and ranged from 1 to 3 sec. The probabilities of all criterion levels P_0–P_X, (where P_X is the probability of the maximum number of spikes occurring in any trial) from the noise [P(false alarm)] and signal [P(hit)] windows were plotted against each other. Consequently, $P(1)$ would be the probability of at least one spike occurring (scanning across all trials) in the respective "hit" and "false alarm" windows. If the maximum number of spikes per trial in a given counting window was 25, then $P_X = P(25)$, and $P(25)$ would represent the probability of at least 25 spikes occurring. Typically, the cumulative probability distributions for both hit and false alarm windows are such that $P(1)$ tends toward 1 and $P(X)$ tends toward zero. Intermediate probability values are obtained for the intermediate criterion levels $P(2)$, $P(3)$, $P(4)$, etc. The "cutoff" or decay of probabilities to zero is faster for false alarm windows because spontaneous activity is less than visually evoked activity. The area (Ag) under this plot of P(hit) versus P(false alarm) is monotonically related to signal detectability (Macmillan and Creelman, 1991). An Ag value of 1.0 thus reflects perfect signal detection, and an Ag value of 0.5 represents an inability of the neuron to detect signal from noise. Comparison of ROC curves and Ag values across control and drug treatment conditions thus provided an unbiased measure of the ability of a pharmacological compound to influence the signal detection capacity of individual cortical neurons. Because a drifting rather than a stationary stimulus was used, the stimulus was not exclusively confined to within the classical receptive field during the visual stimulation period. For the 1–3 sec stimulus times we used, Ag values were not markedly influenced by confining the analysis of the signal window to where the peak visual response exceeds twice the SD of mean background (spontaneous) activity. Indeed, the advantage of ROC is that no assumptions need to be made about when the "response" is significantly above background. As long as the "signal" and "noise" windows are identical in size (duration), the analysis faithfully represented detectability. If the drifting visual stimulus was presented over a larger area so that it overlapped with the receptive field for only a very small fraction of the time, only then was signal detectability significantly underestimated. For the data presented in this paper, we did not adopt such a paradigm. For simple cells, ON–OFF subfield interactions might also result in underestimates of ROC performance; e.g., if a bright bar were passing an OFF region, the firing would dip below spontaneous levels. The spontaneous activity in the vast majority of tested simple cells was low enough so that such ON–OFF interactions did not markedly lead to underestimates of the detection capacity. Because identical duration windows of signal and noise were used in both control and drug conditions, small underestimations of the fidelity of detection did not in any way affect the evaluation of the relative comparison between control and drug conditions. Significance of a change in signal detection was tested on the population of cells using the Wilcoxon signed-rank test.

We also performed CV analysis to quantify the variability of discharge before and during NOS blockade or upregulation. For each cell, under control and drug conditions, the spike count CV,

$$CV_{cnt} = [1 + (1 \div 4n)] \times [(SD \div mean) \times (100)],$$

was calculated (Sokal and Rohlf, 1995), where n is number of trials, and mean is mean number of spikes per trial. The correction factor, $[1 + (1 \div 4n)]$, makes an appreciable difference to the computed CV_{cnt} if a small number of trials (e.g., 5–10) were used. We typically used 30–60 trials per test condition; thus, the correction factor was negligible. After the CV_{cnt} was calculated individually for each cell, for each control and "drug" condition, the significance of a change in the population during NO modulation was evaluated with the Wilcoxon signed-rank test. Because the visually evoked spiking behavior of cortical neurons generally follows renewal (Poisson) statistics where the SD_{cnt} approximately equals the square root of the mean (Shadlen and Newsome, 1998), the CV_{cnt} is expected to change predictably with any changes in the mean visual response. Specifically, as the mean response gets larger the CV_{cnt} decreases, and vice versa. Therefore, we also evaluated whether the measured change in CV_{cnt} during pharmacological application of NO-modulating compounds deviated significantly from that expected from any changes in the mean response. For each cell, we plotted the measured CV_{cnt} against the expected CV_{cnt} for control and various drug conditions (L-ARG, L-MMA, and L-NA iontophoresis; see below) and evaluated whether the slopes of the regression lines between control and drug conditions were significantly increased or decreased.

Two-dimensional spatial receptive field mapping. In several cases, contour maps of the ON and OFF subfields of simple cells were plotted in control conditions and during pharmacological manipulations of the endogenous NO-generating system. Stimuli for these maps comprised of randomly positioned dark and light squares of 0.5–1.0° size and 0.1 sec duration on a 7×7 grid (49 pixels) or 9×9 grid (81 pixels). Luminance and contrast of the background and flashed stimuli were identical to those used for drifting bars (see above). The interstimulus interval was set at 0.5 sec. Responses (spikes) were forward-correlated with the stimuli for each pixel position. Each response pixel value consisted of the mean firing rate (spikes per second) over 16–24 trials windowed over the duration of the stimulus display (0.0–0.1 sec). For each cell, the number of trials was identical for control and drug conditions. Pixel values (spikes per seconds) on the grid were transformed into smooth ON–OFF contour profiles using the Kriging method of interpolation with a linear variogram model (Cressie, 1993). ON and OFF subfields were plotted in graded intensities of red and blue, respectively. For the purposes of comparing the percentage change in the strength of each ON and/or OFF subfield before and during NOS blockade, integrated *xyz* volumes of the ON and OFF subfields were calculated, where the x and y positions corresponded to the spatial coordinates, and the z value represented the evoked response (spikes per seconds). For the 7×7 grid at 1.0×1.0 sized stimulus pixels, ~15 min was required to produce a single ON–OFF receptive field contour map. Larger numbers of grid points and smaller pixel sizes prolonged the mapping time to a maximum of 40 min. For this reason, this technique was used in only a subset of recorded units, all with simple receptive fields.

Pharmacology (iontophoresis). To reduce endogenous cortical NO production, synthetic analogs of arginine (L-NA, 10 mM concentration in the micropipette, pH 6.0; Sigma, St. Louis, MO; or L-MMA, 50 mM concentration in the micropipette, pH 5.5–6.0; Sigma) were iontophoretically administered (10–50 nA). These two compounds inhibit both endothelial NOS (eNOS) and neuronal NOS (nNOS) isoforms, and central excitatory and inhibitory neurons can contain both eNOS and nNOS (Huang et al., 1993; Dinerman et al., 1994; Son et al., 1996). The actual concentrations of the iontophoresed compound in the brain are considerably less than in the micropipette. Intrapipette concentrations of compounds for microiontophoresis in the CNS are typically ≥50 mM (Levine and Jacobs, 1992; Pirot et al., 1992; Cormier et al., 1993; Bond and Lodge, 1995; Budai et al., 1995; Song et al., 1997). Endogenous NO production was increased via iontophoresis (10–50 nA) of the biologically active natural substrate for NOS, L-ARG (50 mM concentration in the micropipette, pH 5.5–6.0; Sigma). Biologically inactive D-forms of arginine analogs (D-ARG, D-MMA, and D-NA) were also tested. Exogenous NO was applied (10–50 nA) using the NO donor molecule DEA-NO (10 mM concentration in the micropipette, pH 8.0–9.0; Cayman Chemical, Ann Arbor, MI). L-Lysine (L-LYS), an amino acid unrelated to the endoge-

Table 1. Summary of database

Pharmacological tests	No. of animals	No. of cells
1. NOS blockade by L-MMA or L-NA	36 (for groups 1–5)	45
2. Endogenous NO upregulation by L-ARG		47
3. Exogenous NO upregulation by DEA-NO		10
4. Combined L-MMA/LNA + L-ARG in same cell		17
5. Combined L-MMA/LNA + DEA-NO in same cell		3
Total	36 cats	122 cells

L-MMA, L-NA, NOS inhibitors; L-ARG, natural substrate for NOS; DEA-NO, NO donor molecule.

nous NO system, but like L-ARG, a basic amino acid, was also tested. We did not perform dose–response tests for these pharmacological agents or attain a saturating effect. Ten to 50 nA ejecting currents were used and assumed to be selective, because D-ARG, D-MMA, and D-NA were without effect in this current range. At 80–120 nA, D-ARG and L-ARG, D-MMA and L-MMA, and D-NA and L-NA modified the response similarly, suggesting nonspecific actions in this higher current range. A similar shift from selective to nonselective effects of *in vivo* iontophoresis of pharmacological compounds has been reported (Do et al., 1994; Williams and Goldman-Rakic, 1995). All iontophoretically administered compounds were prepared in deionized water (OPTIMA; Fisher Scientific, Hampton, NH). DEA-NO was prepared in 10 mM NaOH. One of the barrels of the multipipette assembly was filled with 1 M NaCl and used for current balancing during iontophoresis (Stone, 1985).

Histology and electrode tract reconstruction. At the end of each electrode penetration, an electrolytic lesion was made by passing 5 μA anodal (+) current for 10 sec from the tip of the tungsten recording electrode. As the electrode assembly was slowly retracted out of the cortex, a second lesion was made at half the depth of the tract. At the end of the experiment, the animal was deeply anesthetized with intravenous sodium pentobarbital (40–50 mg/kg; Abbott) and perfused with glutaraldehyde fixative. Tissue blocks containing the electrode tracts were sectioned and alternate slices were stained for either cresyl violet or NADPH diaphorase. Cresyl violet staining allowed the reconstruction of electrode tracts and location of recording sites. NADPH diaphorase staining permitted the identification of NOS-containing neurons and processes (Dinerman et al., 1994). Some animals were not perfused with fixative, and recording sites in these animals were not identified, because the tissue was used for independent electrophysiological slice and biochemical studies.

RESULTS

The role of NO in signal processing in the visual cortex was assessed from electrophysiological recordings obtained from a total of 122 cells in 36 animals (Table 1). Recordings were obtained from cells throughout layers 2–6 of the striate cortex, and the sample included 69 simple cells, 35 complex cells, and 18 cells with unclassified receptive fields, all within 5° of area centralis. The effects of modifying NO production in the visual cortex were not dependent on the subclass of receptive field type (e.g., simple vs complex), the age of the animal, or the cortical layer from which the unit was recorded. Tests for differences in the likelihood and magnitude of effects of L-MMA, L-NA, and L-ARG iontophoresis between kittens and adult cats yielded no significant differences between groups (L-ARG: $z = 0.42$; $n_{\mathrm{KITTEN}} = 28$; $n_{\mathrm{ADULT}} = 36$; $p > 0.05$; L-MMA/L-NA: $z = 0.32$; $n_{\mathrm{KITTEN}} = 33$; $n_{\mathrm{ADULT}} = 30$; $p > 0.05$, Mann–Whitney tests) and simple versus complex cells (L-ARG: $z = 1.02$; $n_{\mathrm{SIMPLE}} = 32$; $n_{\mathrm{COMPLEX}} = 16$; $p > 0.05$; L-MMA/LNA: $z = 0.97$; $n_{\mathrm{SIMPLE}} = 38$; $n_{\mathrm{COMPLEX}} = 24$; $p > 0.05$, Mann–Whitney tests). In cases in which recording sites were successfully reconstructed histologically, the types and frequency of effects were similar in supragranular, granular, and infragranular layers. Therefore, for the purposes of data analysis, the data obtained from the sample of 122 cells were pooled across age, receptive field type, and layer (see Figs. 3, 7; Table 1).

Effects of NO-modulating compounds on the magnitude of the visual response: specificity, reversibility, and uniformity of effects

The effects of iontophoretic application of the natural NOS substrate L-ARG or of the NOS inhibitors L-MMA or L-NA were evaluated for 112 cells. For 20 of those cells, the effects of both facilitation of NO production (by L-ARG or DEA-NO) and inhibition of NO production (by L-MMA or L-NA) were tested. The predominant effect of L-MMA and L-NA (NOS inhibition) was a significant inhibition of the visual response (66% or 43 of 65 cells). In a minority of cells (17% or 11 of 65), the visual response was significantly facilitated. Conversely, enhancement of NO production by L-ARG significantly facilitated the visual response of 23 of 64 (38%) of cells, whereas L-ARG significantly inhibited the visual response of a smaller subset (14% or 9 of 64) of cells. These results are illustrated in Figures 1–3. The summarized data include the effects of both L-ARG and DEA-NO. The effects of both upregulation and downregulation of NO synthesis were assessed using statistical analysis of trial-by-trial spike counts during the time window of stimulus presentation (see Materials and Methods). Typical examples of the effects of modification of endogenous NO production on the visual response of two neurons that had no spontaneous activity are shown in Figures 1 and 2. Data are presented as peristimulus time histograms (PSTHs) and sequential trial-by-trial raster plots (displayed below each PSTH). Compared with the control visual response (Fig. 1*A*), NOS blockade via L-MMA iontophoresis decreased the visual response of the first cell (Fig. 1*B*). Subsequent L-ARG iontophoresis enhanced the visual response of the same cell above control levels (Fig. 1*C*). The adjacent bar graph (Fig. 1*D*) summarizes these effects and shows that NOS inhibition (L-MMA) versus facilitation of NO production (L-ARG) produced significant but opposing changes in the visual response. Like L-ARG, exogenous NO application via iontophoresis of the pH-sensitive NO donor compound DEA-NO also favored enhancement of the visual response (6 of 13 cells vs 3 of 13 cells that had their response reduced by DEA-NO). This finding is consistent with L-ARG exerting its action by facilitating NO production (Malinski et al., 1993). One such example of exogenous NO counteracting the effect of NOS inhibition is shown in Figure 1*E–G*. Compared with control (Fig. 1*E*), NOS inhibition reduced the visual response (Fig. 1*F*), whereas subsequent iontophoresis of DEA-NO potentiated the response above control levels (Fig. 1*G*). The summary bar graph shows that these effects were statistically significant (Fig. 1*H*). Compounds that modified endogenous or exogenous NO production typically took 3–6 min to attain maximal effect and usually returned to control levels within 5–10 min of cessation of the drug application. Although actions of iontophoretically applied conventional neurotransmitters (Stone, 1985;

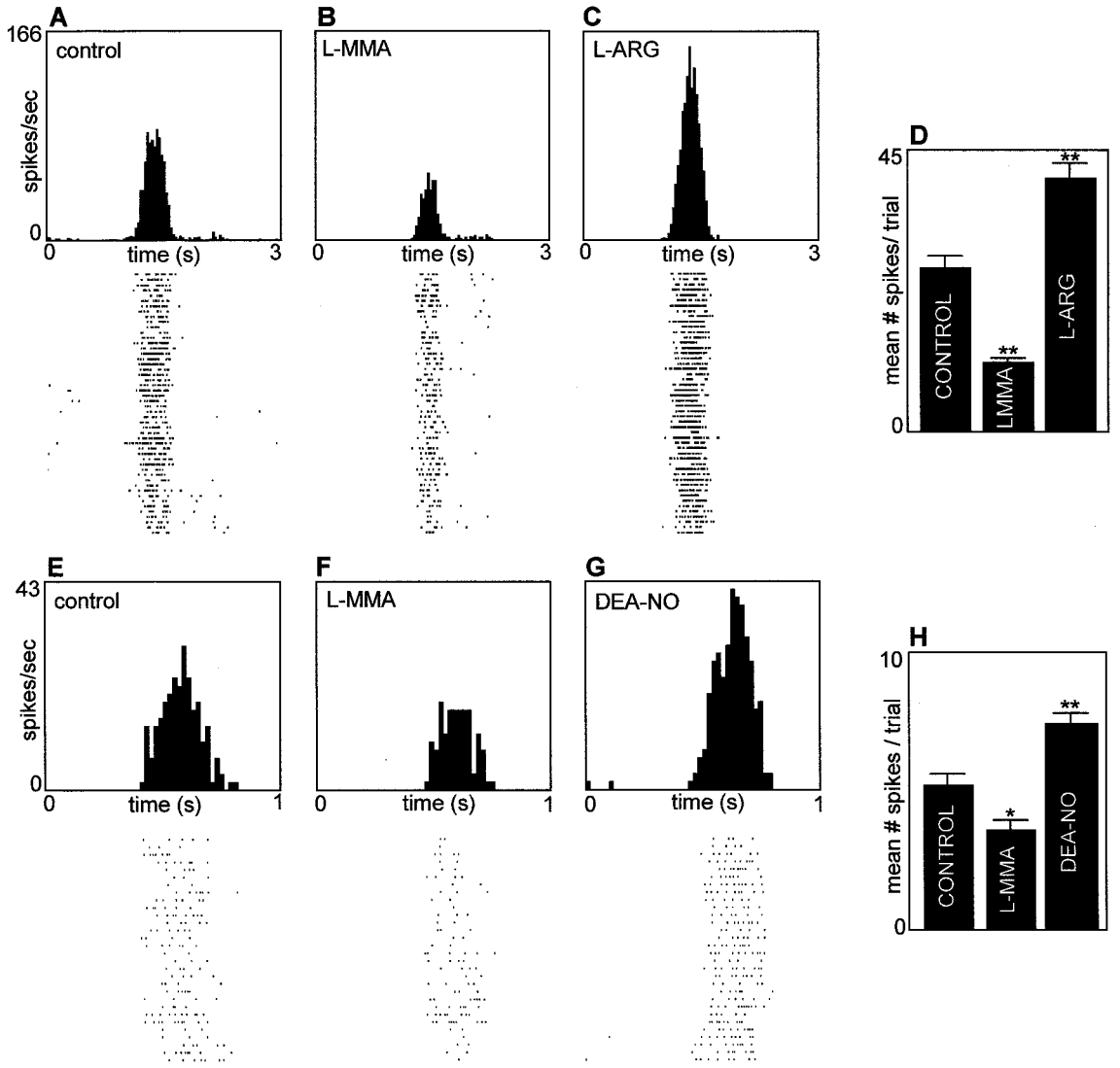

Figure 1. Downregulation and upregulation of NO production produce opposite effects on visually evoked responses from striate cortical neurons. Data for two cells are displayed as PSTHs, individual trial-by-trial raster plots, and summary mean spike count bar graphs. *A–D*, Cell 1: effect of NOS blockade with L-MMA (*B*) and endogenous NO upregulation with L-ARG (*C*). L-MMA reduced the visual response from 26.2 to 11.1 spikes per trial, and L-ARG enhanced the visual response to 40.6 spikes per trial. *E–H*, Cell 2: response during NOS blockade (*F*) and exogenous NO upregulation by DEA-NO (*G*). L-MMA reduced the response from 4.8 to 3.2 spikes per trial, and DEA-NO enhanced the visual response to 7.7 spikes per trial. Effects were significant at $p < 0.005$ (*) and $p < 0.0001$ (**), Mann–Whitney tests. Error bars represent SEM in this and subsequent figures.

Cormier et al., 1993; Bond and Lodge, 1995) that have receptors on the extracellular membrane typically occur in seconds, the arginine analogs require a multistep cascade to exert their action. This includes establishment of an effective local extracellular concentration, relatively slow transport into surrounding cells (Kavanaugh, 1993; Hosokawa et al., 1997), subsequent altered NO synthesis, and diffusion of the NO signal to its targets. Moreover, the analysis requires detection of signal response magnitude over a series of trials often presented at low repetition rates (0.1–0.5 Hz) with inherent response variability. Prolonged effects were evident in six cells in which L-ARG induced a long-lasting enhancement of the visual response (>20 min from termination of the iontophoresis). Attempts to reverse this enhancement with L-MMA in two of the six cells in which long-lasting enhancement occurred were ineffective (results not shown).

Iontophoresis of inactive D-ARG or of the NOS inhibitors D-MMA and D-NA failed to modify the visual response, suggesting that neither the facilitatory effects of L-ARG or DEA-NO nor the inhibitory effects of L-MMA were attributable to iontophoretic currents or vehicle effects such as pH. Examples of this stereoisomer specificity are illustrated for two cells in Figure 2, *A–D* and *E–H*, respectively. Compared with control (Fig. 2*A*), L-ARG enhanced the visual response of the first cell (Fig. 2*B*). After a recovery period, D-ARG application failed to increase the visual response (Fig. 2*C*). The summary bar graph shows that unlike L-ARG, D-ARG did not significantly alter the visual response from control conditions (Fig. 2*D*). Likewise, the inhibition of the visual response by L-MMA (Fig. 2, *F* vs *E*) was specific for the L-form of the NOS inhibitor, because D-MMA (Fig. 2*G*) had no effect. These results are summarized in the bar graph (Fig. 2*H*). Consistent with these results on the specificity of the effects of L-forms of ARG and MMA, L-LYS, an amino acid unrelated to the endogenous NO pathway, did not modify visually evoked

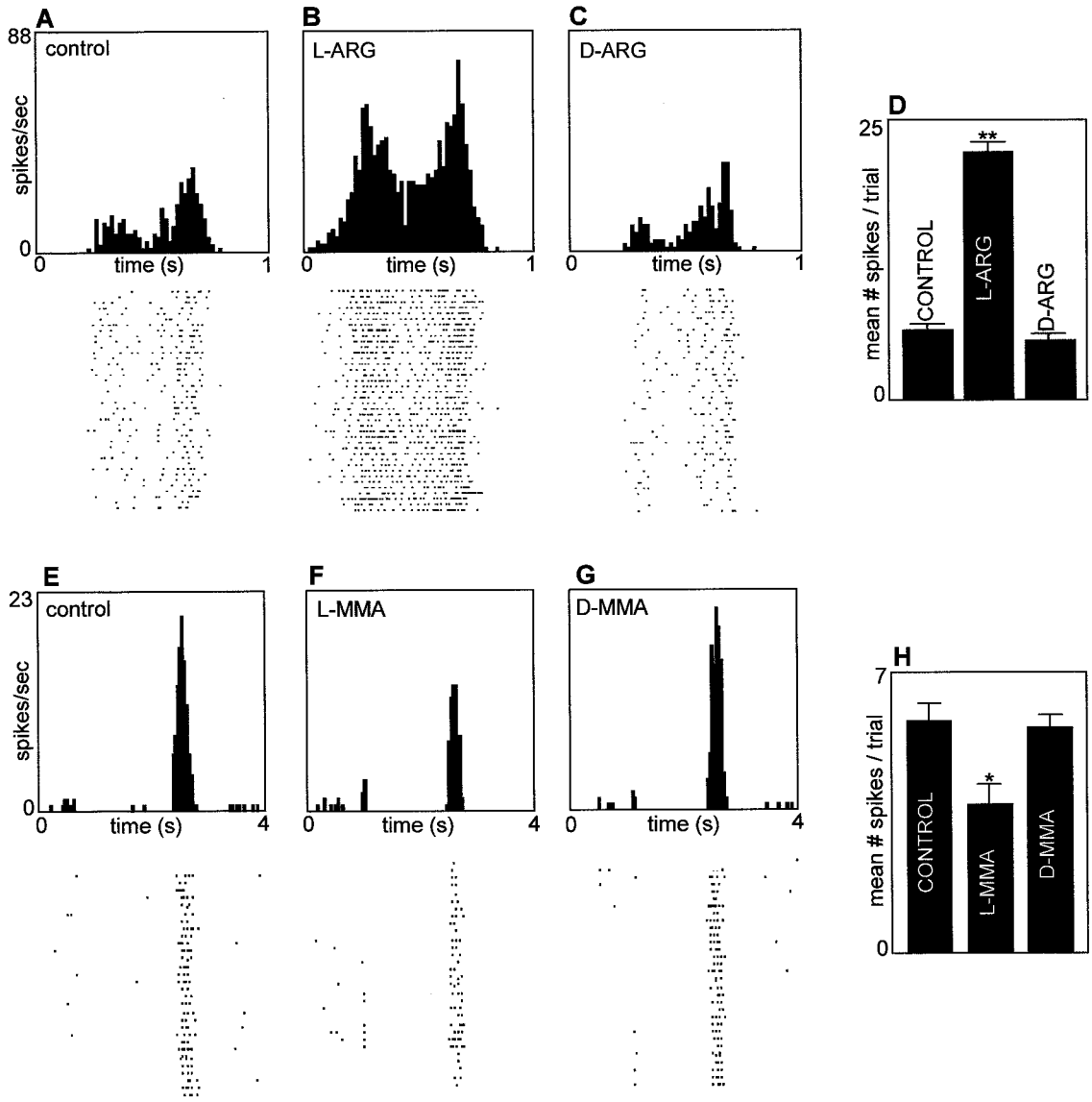

Figure 2. L- but not D-Arginine analogs modify visual responses. Data for two cells are shown. *A–D*, Cell 1. Unlike L-ARG (*B*), which significantly increases the visually evoked response from 6.3 to 22.4 spikes per trial, D-ARG (*C*) has no significant effect (5.4 spikes per trial). *E–H*, Cell 2. Unlike L-MMA (*B*), which significantly reduces the visual response from 5.8 to 3.7 spikes per trial, D-MMA (*G*) has no significant effect (5.6 spikes per trial). Effects were significant at $p < 0.005$ (*) and $p < 0.0001$ (**), Mann–Whitney tests.

responses of this cell or others that had their visual response affected by L-ARG ($n = 5$ cells; see example below).

Overall, downregulation of NO production by NOS inhibition with L-NA or L-MMA reduced the visual responses of the population of cells tested (Fig. 3*A*; 75% or 49 of 65 data points lie below the line of unity) with a significant ($p < 0.005$) negative population effect (see Fig. 3*A* legend for statistical analysis). Conversely, upregulation of NO production by L-ARG or DEA-NO tended to increase the visual responses of the population of cells tested (Fig. 3*B*; 83% or 64 of 77 data points lie above the line of unity) with a significant ($p < 0.005$) positive population effect (see Fig. 3*B* legend for statistical analysis). At the individual cell level, the predominant effect of NOS inhibition by L-NA or L-MMA was a significant reduction of their visual response. Sixty-six percent or 43 of 65 of all cells tested had their visual response significantly reduced by L-NA or L-MMA (Fig. 3*C1*). This represents 80% (43 of 54) of the sample of cells for which NOS inhibition had any statistically significant effect. Conversely, at the individual cell level, although the plurality of cells tested (47%) was not affected by NO upregulation by L-ARG or DEA-NO, the predominant action for those cells whose response was significantly affected was a facilitation of their visual response (38% or 29 of 77 cells; Fig. 3*D, 1*). This represents 71% (29 of 41) of the sample of cells for which NO upregulation by L-ARG or DEA-NO had any significant effect. The magnitude of these changes for each case is summarized for NOS inhibition and NO upregulation in Figure 3, *C, 2*, and *D, 2*, respectively. In 20 cells (Table 1, see groups 4 and 5), the effects of increasing *and* decreasing NO were sequentially tested on the same cell by L-ARG or DEA-NO and L-NA or L-MMA application, respectively. Both manipulations had significant effects on individual cells in 7 of 20 cases (Fig. 1*B*,*C*,*F*,*G*). These effects of increasing versus decreasing NO always were complementary ($n = 7$ of 7) and were consistent with NO enhancing the visual response ($n =$

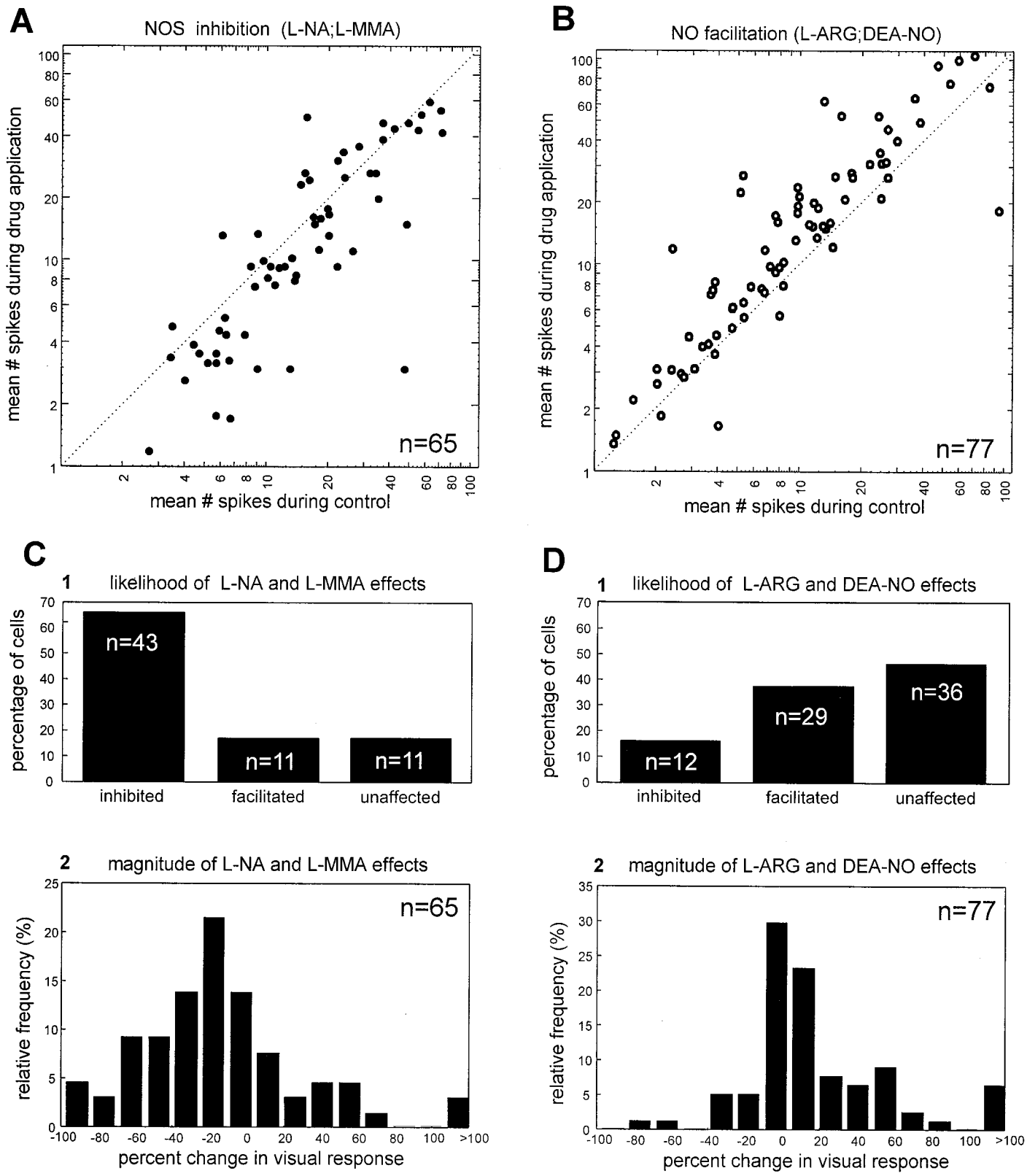

Figure 3. Summary of mean visually evoked responses during control versus NOS downregulation and upregulation. *A*, Scatterplots of mean spike counts per trial during control versus during NOS blockade via L-MMA or L-NA iontophoresis for all tested cells. Each point (*filled circle*) represents the control versus test response for an individual cell. More points lie below ($n = 49$) the unity line (*dotted*) than above ($n = 16$) it. For the population of tested cells, iontophoresis of NOS inhibitors significantly decreased the mean number of spikes (Wilcoxon $Z = 3.103$; $p < 0.005$; $n = 65$). *B*, Scatterplot of mean spike counts during control versus endogenous NO upregulation via L-ARG iontophoresis or exogenous NO application via DEA-NO iontophoresis. Although many points lie at unity, the population as a whole shows a significant increase in the mean spike count during NO upregulation (Wilcoxon $Z = 2.324$; $p < 0.005$; $n = 77$). *C*, Frequency distribution histograms summarizing the likelihood (*1*) and (*Figure legend continues*)

6 of 7). In no case did NO enhancement by provision of the natural NOS substrate L-ARG or by provision of exogenous NO by DEA-NO iontophoresis cause the same effect as NO reduction by NOS inhibition with L-MMA or L-NA iontophoresis ($n = 0$ of 20). The combined n in Figure 3*, C, 2*, and *D, 2*, is 142, although only 122 cells were tested, because in 20 cases both the effects of NOS inhibition and NO upregulation were evaluated.

Effects of NO-modulating compounds on signal detection

Trial-by-trial analysis of spike counts during visual stimulation and statistical comparisons of their means before and during iontophoresis of NO-modulating compounds were used for both nonspontaneously and spontaneously active cells. This method accounted for the changes in neuronal discharge in neurons lacking spontaneous activity. However, it did not account for all changes seen in some neurons that were spontaneously active. This is attributable the ability of NO-modulating compounds to modify both spontaneous and visual activity. ROC analysis accounts for relative changes in visual stimulus-evoked and spontaneous activity and therefore provides an index of the ability of neurons to distinguish signal from noise (see Materials and Methods). We did not preselect a minimum acceptable level of spontaneous firing suitable for ROC analysis, because this criterion level was likely to change with various pharmacological manipulations. Therefore, ROC analysis was performed on all 122 neurons (from groups 1–5 in Table 1) in which L-ARG, L-MMA, L-NA, and DEA-NO were applied. Fifty-four percent (66 of 122) of cells were spontaneously active under control (drug-free) conditions. The mean rate of spontaneous discharge for all 66 cells together was 7.8 spikes/sec. Because of the overlapping data from group 4 (cells in which the effects of L-MMA/L-NA and L-ARG were tested) and group 5 (cells in which the effects of L-MMA/L-NA and DEA-NO were tested) (Table 1), a total of 142 data sets were available for ROC analysis.

ROC analysis revealed that NOS blockade reduced signal detection and endogenous NO upregulation enhanced the detection capacity. Examples of these effects from six cortical neurons are shown in Figures 4–6. The contribution of endogenous NO production to signal detection is indicated by the ability of NOS inhibition (via L-MMA iontophoresis) to reduce the Ag value of the ROC (examples are illustrated in Fig. 4*A–D*,*E–H*). NOS blockade decreased the ability of these two cortical neurons to detect the visual stimulus, because their Ag values decreased from 0.82 (Fig. 4*C*) to 0.59 (Fig. 4*D*) and from 0.88 (Fig. 4*G*) to 0.49 (Fig. 4*H*), respectively. As is evident in the PSTHs and raster plots for these particular cells, in one case (Fig. 4*A–D*), the decrease in signal detection was primarily attributable to a change in the discharge during visual stimulation (1–3 sec) and not the spontaneous activity (0–1 sec). However, in the second example (Fig. 4*E–H*), the decrease in the ROC was attributable to a change in the spontaneous activity and a change in the visual response. However, the effect of NOS inhibition by L-MMA on the visual response was greater, thus effectively decreasing the signal-to-noise ratio. In a complementary manner, L-ARG increased cell signal detection, as shown in Figure 5. Compared with the control period (Fig. 5*A*), L-ARG iontophoresis (Fig. 5*B*) decreased the spontaneous discharge (time, 0–1 sec) without reducing the visual response (time, 1–3 sec). The raster plots illustrate a transformation by L-ARG of the cell response to one of increased regularity. Moreover, the ability of this neuron to detect the visual stimulus increased. This increase in signal detection was confirmed with ROC curve fitting for control (Fig. 5*C*) and L-ARG (Fig. 5*D*) conditions. The Ag of the ROC plot increases from 0.88 to 0.99 with L-ARG iontophoresis (Fig. 5*C*,*D*). Thus, L-ARG changed the profile of the visual response in this cell to provide near-perfect signal detection (Ag close to 1.0). D-ARG had no effect (data not shown). A second example of the capacity for upregulation of endogenous NO production by L-ARG to enhance signal detection is illustrated in Figure 5*E–H*. The enhancement of the signal detection of the cell (Ag increases from 0.77 to 0.98) is attributable to a combination of effects, an increase in the magnitude of the visual response and a decrease of the spontaneous discharge. The capacity of L-ARG to enhance signal detection could also occur without obvious effects on the visual response. The example illustrated in Figure 6*A–D* illustrates that L-ARG could also act by predominantly reducing the spontaneous discharge alone. In this case, L-ARG increased Ag from 0.87 to 0.98, eliminating much of the spontaneous activity, except for occasional burst discharges (see raster in Fig. 6*B*).

Because L-ARG was capable of facilitating signal detection by neurons in response to stimuli that under control conditions elicited reasonably strong responses to our optimal stimulus configuration, we posited that L-ARG might be capable of enhancing detection of weak, nonoptimally configured stimuli. An example of a response to such a nonoptimal visual stimulus is illustrated in Figure 6*, E*, *F*, *H*, and *I*. Note that the response consists of only one or two spikes per trial nested in the surrounding spontaneous discharge (see raster in Fig. 6*E*). A vigorous response emerges from the background during L-ARG iontophoresis (Fig. 6*F*), however. In this example, the specificity of the L-ARG effect also is illustrated. As shown in Figure 6*, G* and *J*, iontophoresis of the related amino acid L-Lysine has no effect on the response of the cell or its signal detection (the Ag returns to near control levels, 0.58).

ROC analysis for the entire sample under the different conditions (NOS blockade vs NO upregulation) is summarized in Figure 7*A* as raw ROC values. The primary effect of NOS blockade was a reduction in signal detectability (*open circles* below line of unity), whereas NO upregulation by L-ARG increased detection (*closed circles* above line of unity). The population difference was significant (NOS inhibition reduced the ROCs; $p < 0.005$; NO upregulation by L-ARG increased the ROCs; $p < 0.05$; see Fig. 7 legend). Moreover, because many cells with no spontaneous activity already had near-perfect signal detection (Ag = 1.0), L-ARG iontophoresis could not further enhance their ROC val-

←

magnitude (*2*) of the effect of NOS inhibitor application. Most cells (43 of 65 or 66%) showed a significant reduction of the visual response. Seventeen percent ($n = 11$ of 65) of the tested cells showed the opposite effect (*1*). Of the 54 of 65 cells (83%) that had their visual response significantly affected by NOS inhibition, the magnitude of the predominant (inhibitory) effect ranged from −11 to −99%, and the distribution of the percent change in the visual response was shifted to the left of 0% (see *2*). *D*, Cells that were significantly affected by NO upregulation either by exogenous NO (via DEA-NO) or by endogenous NO (via L-ARG) are grouped together. The responses of 53% (41 of 77) of the cells were significantly affected by NO upregulation. In 29 of 41 (71%) of these cases, the visual response of the cell was significantly enhanced (*1*), the magnitude of the enhancement ranging from +10 to +250%. The distribution of the percent change in the visual response during NO upregulation was shifted to the right of 0% (see *2*).

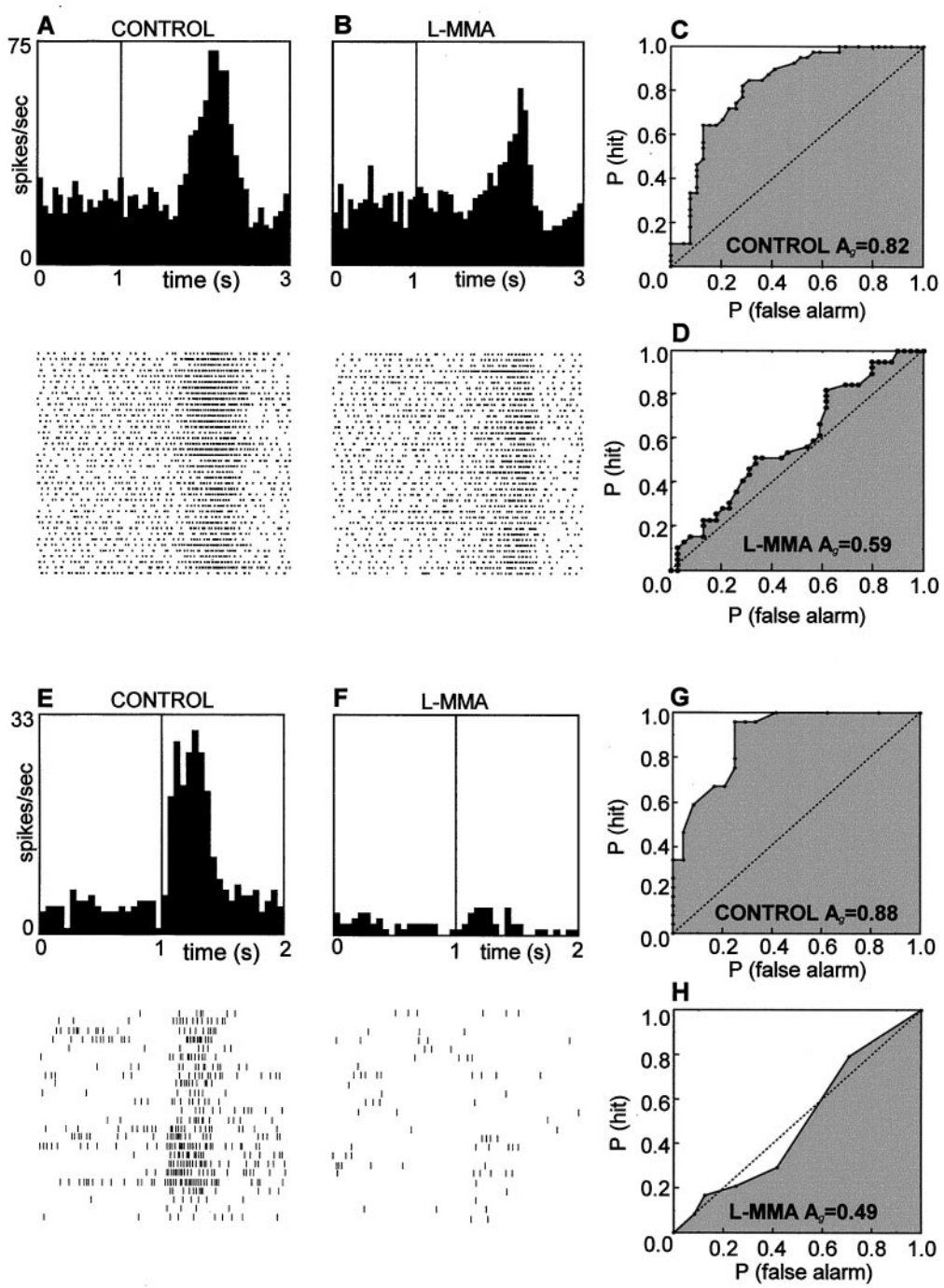

Figure 4. NOS inhibitors decrease the signal detection by individual cortical neurons. Responses are shown for two neurons [cell 1 (*A–D*) and cell 2 (*E–H*)]. Conventions are as in previous figure, except the 0–1 sec period represents spontaneous activity (no stimulus is present, but the viewing screen is homogeneously illuminated at the same background luminance level as when a stimulus is present), and the 1–3 sec (or 1–2 sec in cell 2) period is when the stimulus drifts through the receptive field. Signal detection is plotted as an ROC curve (*C*, *D*) and quantified as the Ag. In both cells, iontophoresis of the NOS inhibitor L-MMA decreases signal detection, which is shown as a decrease in the area under the ROC curve. In cell 1, L-MMA decreases the ROC (or Ag) from 0.82 to 0.59 (*C*, *D*). In cell 2, L-MMA decreases the Ag from 0.88 to 0.49 (*G*, *H*). Note that although L-MMA decreased signal detection in both cells, the degree of change in the spontaneous activity during L-MMA application was variable between the various cortical cells recorded. In the first cell (*A*, *B*) the spontaneous activity was unaffected, whereas in the second cell (*E*, *F*), the spontaneous activity and visual activity were reduced. Nevertheless, the effect of L-MMA on the visual response was greater than that on the spontaneous discharge, thus effectively decreasing the signal to noise.

ues, thus further diluting the apparent population differences in the mean change in the ROC values. However, ROCs of individual cells were changed by amounts ranging from +7 to −49% (NOS inhibition by L-MMA) and −9 to +72% (NO upregulation by L-ARG).

Effects of NO-modulating compounds on the coefficient of variation of the visual response

For the large number of cells (46%) that already displayed perfect signal detection during control conditions primarily because of

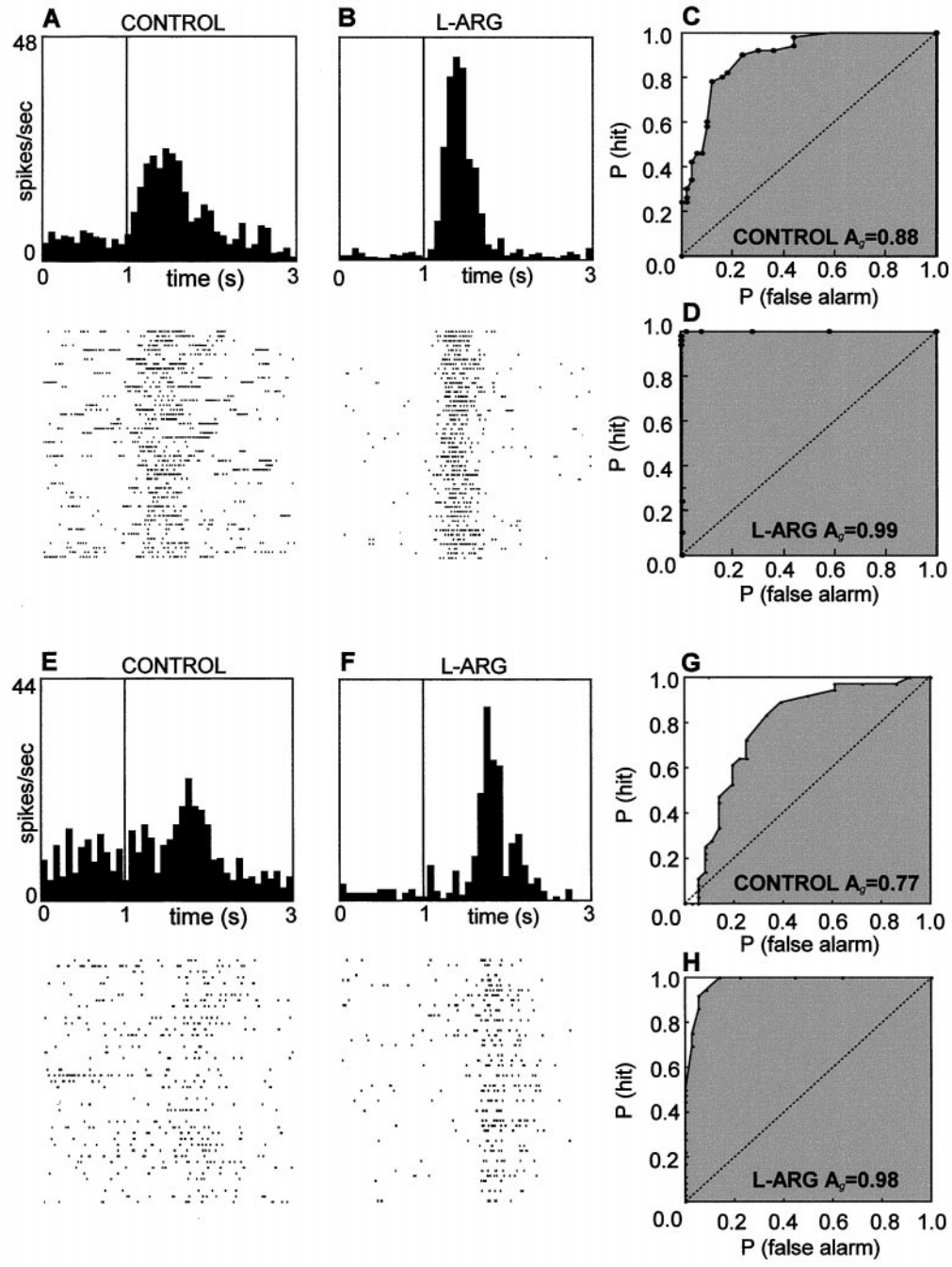

Figure 5. L-ARG increases the signal detection by cortical neurons. Responses are shown for two neurons [cell 1 (*A–D*) and cell 2 (*E–H*)]. In both cells, time 0–1 sec represent spontaneous discharge (no visual stimulus present) and 1–3 sec represent visually evoked activity. L-ARG increases signal detection in cell 1 from 0.88 to 0.99 (*C*, *D*) and in cell 2 from 0.77 to 0.98 (*G*, *H*). In both cases, L-ARG increases signal detection by simultaneous increases in the magnitude of the visual response and decreases in the magnitude of the spontaneous discharge.

their lack of spontaneous discharge, ROC methods were not useful in assessing a change in their signal detection. However, changes in the trial-by-trial variability of visually evoked responses may also relate to changes in signal detection (Godwin et al., 1996; de Ruyter van Steveninck et al., 1997; Berry and Meister, 1988; Shadlen and Newsome, 1998). The SD of visual responses with respect to the mean response was calculated before and during NOS manipulation as the CV of the number of spikes per trial, CV_{cnt} (see Materials and Methods). CV_{cnt} analysis is applicable in cases of high and low signal detection, because it measures differences in SD with respect to the mean response, both for cells that are spontaneously active and those that are not spontaneously active.

For some cells in which L-ARG was applied, the increase in signal detection was associated with a decrease in the CV_{cnt} of the evoked discharge. An example of this is illustrated in Figure 5*A–D*, where L-ARG increased the Ag from 0.88 to 0.99 and the CV_{cnt} of the trial-by-trial spike counts decreased from 48 to 36%. In addition, in this example, the trial-by-trial responses showed less temporal jitter and spontaneous bursting during L-ARG

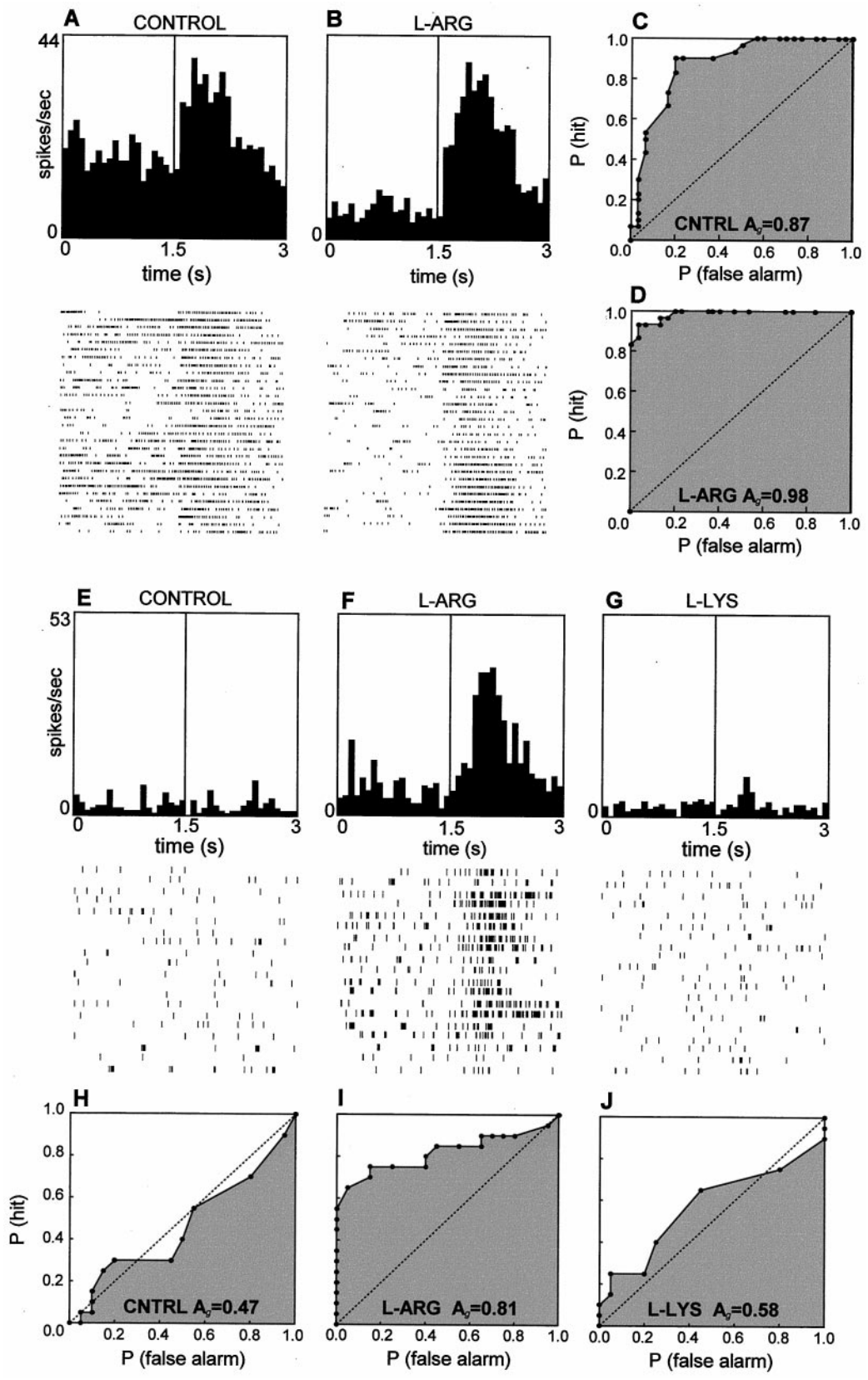

Figure 6. L-ARG but not L-LYS increases signal detection. Responses are shown for two neurons [cell 1 (*A–D*) and cell 2 (*E–J*)]. In both cells, time 0.0–1.5 sec represent spontaneous discharge, and 1.5–3.0 sec represent visually evoked activity. In the first cell (*A–D*), L-ARG increases signal detection from 0.87 to 0.98, primarily by a decrease in the spontaneous discharge and not an increase in the magnitude of the visual response. In the second example (*E–J*), the neuron was weakly responsive to visual stimuli in control conditions (see *E*) as reflected by a low level of signal detection (Ag = 0.47; see *H*). L-ARG increases signal detection to 0.81 by a relative increase in visual versus spontaneous activity (see *F*, *I*). L-LYS, an amino acid unrelated to the L-ARG nitric oxide pathway, did not produce a comparable increase in the signal detection; Ag = 0.47 in control versus 0.58 with L-LYS (see *G*, *J*).

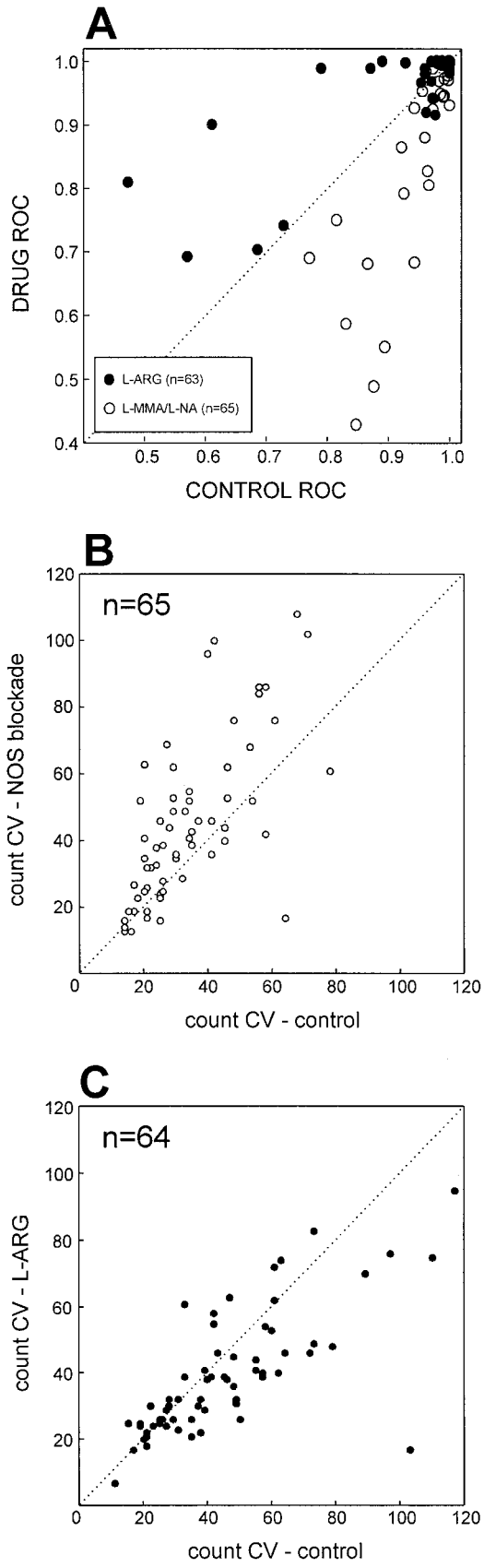

Figure 7. Summary of ROC and CV analysis. *A*, Scatterplot of ROC values for individual cells before and during NOS blockade (*open circles*) and enhanced endogenous NO production via L-ARG application (*filled circles*). Each point represents the ROC value for a single cell during control versus iontophoresis conditions. NOS blockade via L-MMA or L-NA reduced the ROC values, and thus signal detection (Wilcoxon $Z = 3.855$; $p < 0.0005$; $n = 65$) and endogenous upregulation with L-ARG increased signal detection (Wilcoxon $Z = 2.208$; $p < 0.05$; $n = 63$). *B*, *C*, Scatterplots of the CV values for spike counts for individual cells during control versus endogenous NO downregulation (*C*) and upregulation (*D*). NOS blockade significantly increased the population spike count CV (Wilcoxon $Z = 5.136$; $p < 0.0001$; $n = 65$), and L-ARG significantly decreased the spike count CV (Wilcoxon $Z = 3.019$; $p < 0.005$; $n = 64$).

iontophoresis. CV_{cnt} analysis was performed on all cells in groups 1–5 (Table 1) in which endogenous NO production was upregulated or downregulated. NOS blockade via L-NA or L-MMA significantly increased CV_{cnt} (Fig. 7*B*), whereas endogenous NO upregulation by L-ARG iontophoresis significantly decreased CV_{cnt} (Fig. 7*C*). The small size of the DEA-NO sample negated analysis for this group. The change in signal detection was negatively correlated with CV_{cnt} ($r = -0.473$; $p < 0.0001$; $n = 129$; data not shown). The sample size for the correlation was higher ($n = 129$) than count CV analysis as L-NA, L-MMA, and L-ARG cases were combined. The CV_{cnt} is expected to decrease when the response mean increases (and vice versa), but the change attributable to manipulating NO levels was somewhat greater than that predicted by the change in the mean response alone.

Insights into mechanisms of NO actions—differential responses in simultaneously recorded neighboring neurons and receptive field subfields: blood flow effects

Aside from the various neuronal sources and targets of NO (Snyder, 1992; Garthwaite and Boulton, 1995), NO produced from endothelial cells (and neurons) can dilate blood vessels (Moncada et al., 1991). Consequently, it is possible that the effects of microiontophoretic applications of L-ARG and L-MMA occurred via indirect effects of NO on the vascular smooth muscle (Moncada et al., 1991; Irikura et al., 1995; Moncada, 1997) from NO biosynthesis in endothelial cells lining the smooth muscle of the vasculature or from neurons. eNOS and nNOS isoforms were originally thought to be mutually exclusive to endothelial cells and neurons, respectively. However, both isoforms may be expressed in CNS neurons (Huang et al., 1993; Dinerman et al., 1994), and specific pharmacological tools to selectively block NO production in either neurons or vasculature are not available.

Our iontophoresis experiments cannot differentiate between the actions of NO on the vasculature (and thus indirectly on neurons) versus direct actions on neurons *in vivo*. However, certain predictions can be made about how such effects may manifest. We therefore used three additional experimental protocols to help discriminate between NO actions. These included evaluation of (1) the effect of NO-modulating compounds on responses of simultaneously recorded neighboring cells at the same recording site, (2) the effect of NO-modulating compounds on the spatial profile of ON and OFF subregions of individual simple cell receptive fields, and (3) enhancement of cerebral blood flow by 5% CO_2 inhalation. The rationale for the first two experiments is that if the ability of NO to modify neuronal visual responses (such as response magnitude and signal detection) were primarily attributable to an indirect general effect of increasing blood flow in the area subject to iontophoretic delivery of the NO-modulating compounds, these effects should be "mass action"

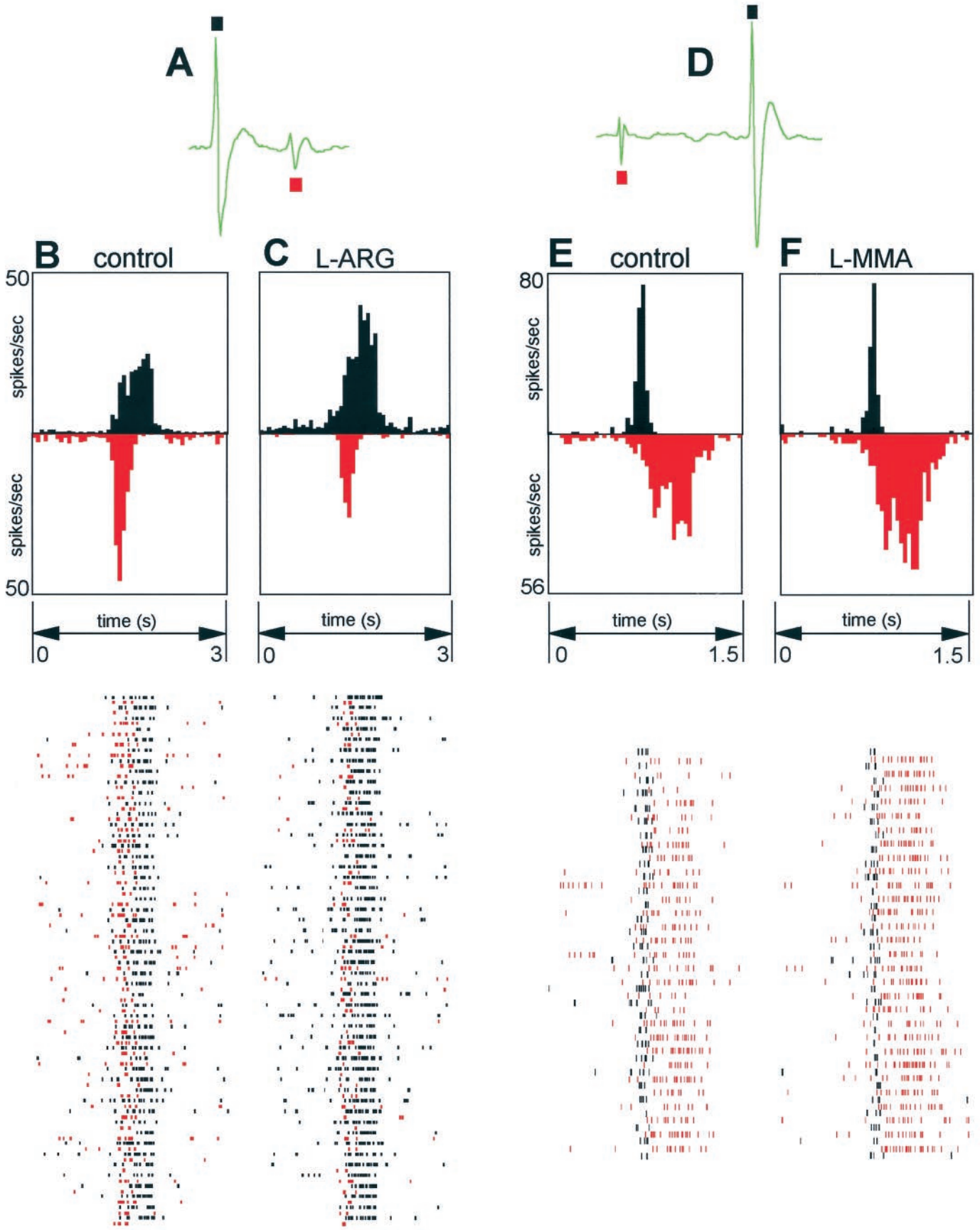
A
D
B control
C L-ARG
E control
F L-MMA
50
spikes/sec
spikes/sec
50
time (s)
0
3
time (s)
0
3
80
spikes/sec
spikes/sec
56
time (s)
0
1.5
time (s)
0
1.5

in nature, and the compounds should not differentially affect neighboring cells or neighboring synapses on the same cell. Toward that end, we took advantage of our observation that although NO-modulating compounds have a predominant effect, they sometimes have an opposing effect on different cells recorded at different sites. By designing the experiment to record from neighboring neurons simultaneously while delivering an NO-modulating compound at that site, we could evaluate whether a mass action secondary to the ability of NO to enhance blood flow was likely to be responsible for the effects on the visual responses of the cells.

Two examples of simultaneous recordings from two pairs of neighboring neurons during L-ARG and L-MMA iontophoresis, respectively, are shown in Figure 8. The waveform traces in *green* and the discrimination between large (*black*) and small (*red*) units are shown in Figure 8, *A* and *D*, for the two recording sites. The PSTHs and raster plots from each of the two neurons for the L-ARG experiment and the L-MMA experiment are shown in *black* and *red* in Figure 8, *B* and *C* and *E* and *F*, respectively. In the L-ARG iontophoresis experiment (Fig. 8*A–C*), for the neuron shown in *black*, the visual response was facilitated (Fig. 3*D, 1*, *2*). At the same time, the response of the other neighboring neuron, shown in *red*, was reduced, demonstrating the rarer effect (Fig. 3*D, 1*, *2*) of NO upregulation. In the L-MMA iontophoresis experiment (Fig. 8*D–F*), for the neuron shown in *black*, the visual response was inhibited, typical of the predominant effect of NOS inhibition (Fig. 3*C, 1*, *2*). Concurrently, the visual response of the neuron shown in *red* was facilitated, indicative of the rarer effect (Fig. 3*C, 1*, *2*) of NOS inhibition. We analyzed 13 such pairs of visually evoked responses from neighboring cells. Three of 13 pairs showed opposing effects during NO manipulation. Such opposing effects are unlikely to be attributed to local uniform changes such as would be predicted if the predominant effect of the NO manipulations on neuronal responses were solely the result of the indirect effect of NO on neurons secondary to its vascular relaxing effects. Using a similar rationale, we reasoned that if the predominant general effect of NO on visual cortical neuron responsiveness was secondary to its local vascular actions, then L-ARG or L-MMA iontophoresis should have similar effects on neighboring synapses. Because current models of the receptive field organization of visual cortical simple cells incorporate differential synaptic input from on-center and off-center geniculocortical afferents onto the simple cell, providing its characteristic spatially separate ON–OFF substructure (Reid and Alonso, 1995; Ferster et al., 1996; Chung and Ferster, 1998), we made use of this observation in our studies.

Using a different stimulus set, i.e., small stationary flashes of randomly positioned visual stimuli versus drifting bars of light, two-dimensional (2D) spatial receptive field maps were constructed before and during NOS inhibition in six simple cells to determine whether the contribution of NO to the ON and OFF subfields of the simple cell receptive fields was equally and generally affected or differentially modified. An example of this type of analysis is shown in Figure 9*A*. NOS blockade selectively reduced the strength of the ON subfield (shown in *red*) by 40% ($Z = 2.00$; $n = 49$ pixels; $p < 0.05$, Wilcoxon signed-rank test); the OFF subfield (shown in *blue*) was not affected (5% change; $Z = 1.68$; $n = 49$ pixels; $p > 0.05$, Wilcoxon signed rank test). This specific effect of NOS blockade on a single subfield is not likely to have occurred via L-MMA compromising blood flow, because both subfields would be expected to be equally affected, and the receptive field structure would likely be severely disrupted. In four of six cells tested in this manner, NOS blockade reduced the response in one or more subfields. The opposite effect, in which at least one subfield was enhanced by NOS blockade, was found in the remaining two cells. One such example is given in Figure 9*B*. Here, NOS inhibition by L-MMA enhanced the strength of both the ON and OFF subfields (Fig. 9*B, 2*) but by different amounts, 95% ($Z = 2.56$; $n = 49$ pixels; $p < 0.05$, Wilcoxon signed-rank test) and 75% ($z = 3.77$; $n = 49$ pixels; $p < 0.0005$, Wilcoxon signed-rank test), respectively. Subsequent L-ARG application antagonized this effect and reduced the magnitude of the ON and OFF subfields (Fig. 9*B, 3*) by 51% ($Z = 3.20$; $n = 49$ pixels; $p < 0.005$, Wilcoxon signed-rank test) and 36% ($Z = 2.45$; $n = 49$ pixels; $p < 0.05$, Wilcoxon signed-rank test), respectively.

Another strategy for evaluating whether the effects of iontophoresis of NOS inhibitors and L-ARG might be secondary to vascular actions is to intentionally change cerebral blood flow with another method. CBF was increased with inhalation of 5% CO_2. This protocol consistently increased CBF (as measured by surface LDF) by an average of 25% from baseline. Together with the LDF measure, the visually evoked neuronal discharge was recorded in five cortical neurons before and during enhanced CBF induced by inhalation of 5% CO_2. A typical example is shown in Figure 10. Compared with baseline (Fig. 10*A*), hypercapnia (via 5% CO_2) increased CBF (Fig. 10*B*). The neuronal visual responses (PSTHs) during control conditions and hypercapnia are shown in Figure 10, *C* and *D*, respectively, and individual records from single trials are illustrated in Figure 10, *E* and *F*. During hypercapnia, overall neuronal activity increased, but the signal (visually evoked activity, 0–3 sec window) relative to noise (maintained activity in the absence of visual stimulation, 3–6 sec window) decreased. ROC analysis was used to quantify the change in signal detection. ROC plots show the detection capacity decreased from 0.96 in the control period (Fig. 10*F*) to 0.63 during CO_2 inhalation (Fig. 10*F*).

←

Figure 8. Opposite neuronal effects on NOS manipulation recorded simultaneously from pairs of different cortical neurons at the same recording site. First pair shown in *A–C*. *A*, Waveforms (*green*) of simultaneously recorded action potentials (spikes) from two neighboring cells. The occurrences of spikes from these two cells are indicated in *black* and *red*. *B*, *C*, PSTH and raster plots during control conditions (*B*) and L-ARG iontophoresis (*C*). PSTH of the smaller unit (*red*) is shown inverted below the larger unit (*black*) response. Raster plots for the two units are overlaid but slightly vertically offset for clarity. L-ARG increased the visual response for the *black* cell from 11.4 to 18.3 spikes per trial ($p < 0.001$, Mann–Whitney). In the other simultaneously recorded unit (*red*), L-ARG decreased the response from 9.3 to 5.8 spikes per trial ($p < 0.001$, Mann–Whitney). Opposing effects recovered within 10 min of termination of the L-ARG iontophoresis (results not shown). Both cells in this first pair had near-perfect signal detection (Ag of 0.99 and 0.95, as evaluated by ROC) during control conditions. Small changes in spontaneous activity were evident with L-ARG, but ROC values changed by <3%. A second pair of simultaneously recorded neurons is shown in *D–F*. *E*, *F*, PSTH and raster plots during control conditions (*E*) and L-MMA iontophoresis (*F*). L-MMA significantly decreased the visual response in the *black* cell from 6.0 to 4.7 spikes per trial ($p < 0.05$, Mann–Whitney) but simultaneously increased the visual response in the *red* cell from 11.6 to 16.7 spikes per trial ($p < 0.0005$, Mann–Whitney). ROCs were largely unaffected in both cells.

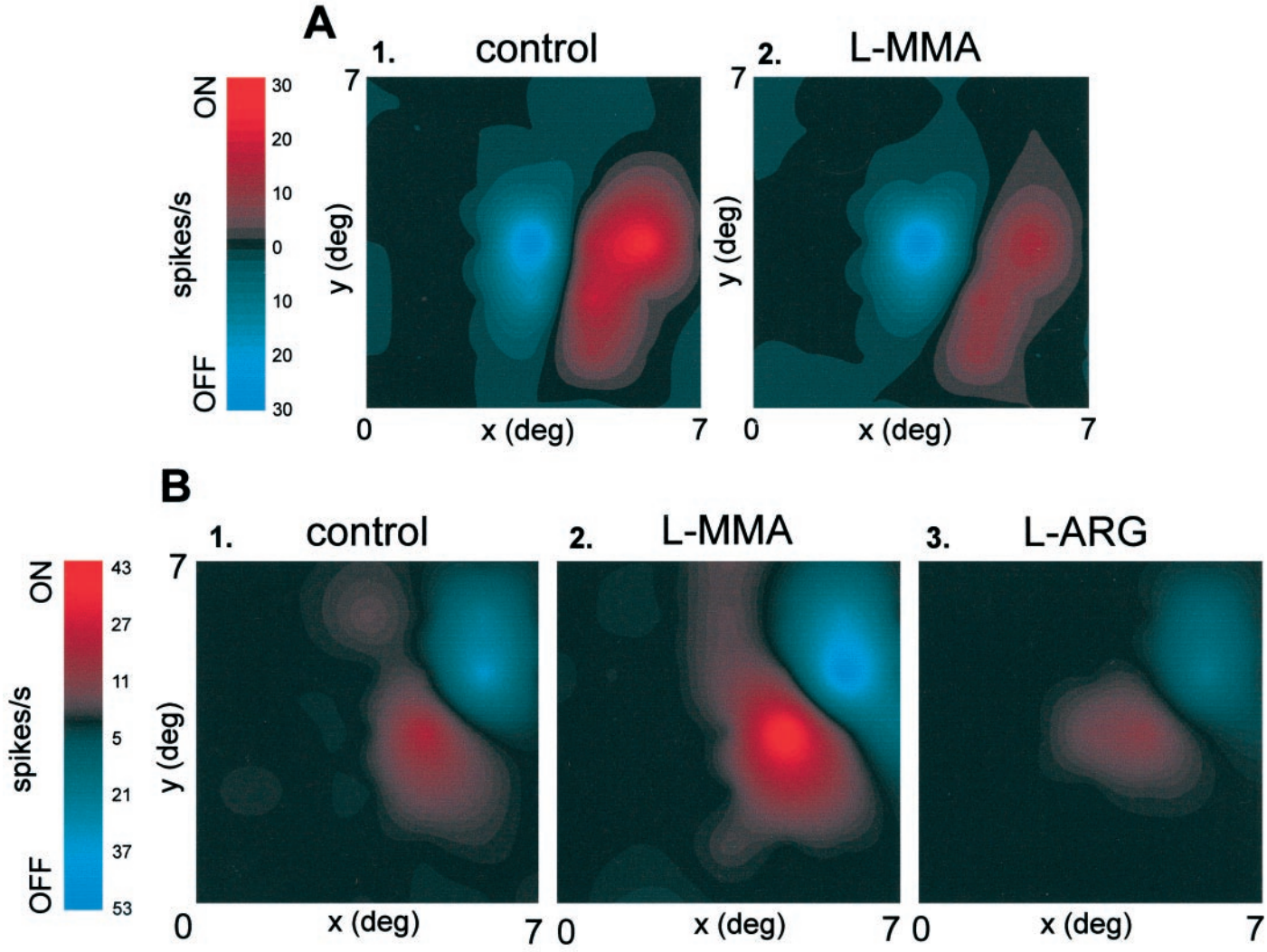

Figure 9. Effects of modification of endogenous NO levels on the 2D spatial profile of simple cell receptive fields. *A*, Cell 1. 2D ON–OFF maps before (*1*) and during NOS blockade with L-MMA (*2*). ON and OFF subfields are shown in *red* and *blue*, respectively (see Materials and Methods). The *brighter* the *red* or *blue*, the stronger the magnitude of the ON or OFF response. The overall strength of the ON subfield was reduced during L-MMA iontophoresis. The strength of the OFF subfield was not significantly affected. Thus, NO selectively facilitated the ON subfield of this cell. *B*, Cell 2. ON–OFF maps during control (*1*), NOS blockade (*2*), and L-ARG application (*3*). Color scheme as in cell 1. In this cell, the strength of both the ON and OFF subfields was markedly changed after NOS manipulation. L-MMA increased the strength of the ON and OFF subfields. L-ARG antagonized this effect and further reduced the ON and OFF subfields. Thus, NO appears to have inhibited the strength of the ON and OFF subfields in this cell. Note that the scale bar for both ON and OFF subfields are plotted from zero to positive values. ON and OFF subfields were plotted from the response to separate presentations of light and dark stimuli, respectively (see Materials and Methods). Therefore, OFF subfield responses were also plotted from zero to positive.

DISCUSSION

Our primary observations are that local application of the natural NOS substrate L-ARG or application of exogenous NO facilitate the visual response of many (38% or 29 of 77) cortical neurons, whereas the complementary protocol of locally inhibiting endogenous cortical NOS reduces the visual responses of most (66% or 43 of 65) cortical neurons. These results are consistent with the effects of these compounds being mediated by NO for several reasons: exogenous NO application by DEA-NO mimics provision of NOS substrate (L-ARG); NOS inhibition by L-MMA or L-NA has a complementary pattern of effects to L-ARG administration; and the effects of L-ARG and DEA-NO are consistently overcome and reversed by NOS inhibition and vice versa in individual cells. The conclusion that the effects of these compounds are exerted specifically through the actions of NO versus other nonspecific mechanisms of the iontophoresis procedure is also consistent with our observations that neither their D-isomers nor L-lysine have an effect on the same cells. For cortical neurons that are spontaneously active, ROC analysis provided a richer description of the role of NO in sensory signal processing. L-ARG increases signal detection in a subset of these neurons because of increases in the visual response, decreases in spontaneous activity, or both. In cells that have either high or low levels of signal detection, similar enhancement of endogenous NO production via L-ARG also decreases the coefficient of variation of evoked neuronal discharges. Although the precise signal transduction pathway for the effects of NO on visual cortical neurons responses *in vivo* is uncertain, our results are consistent with observations *in vitro* of NO having direct synaptic effects. They do not support an indirect general vascular effect as the primary or sole mechanism

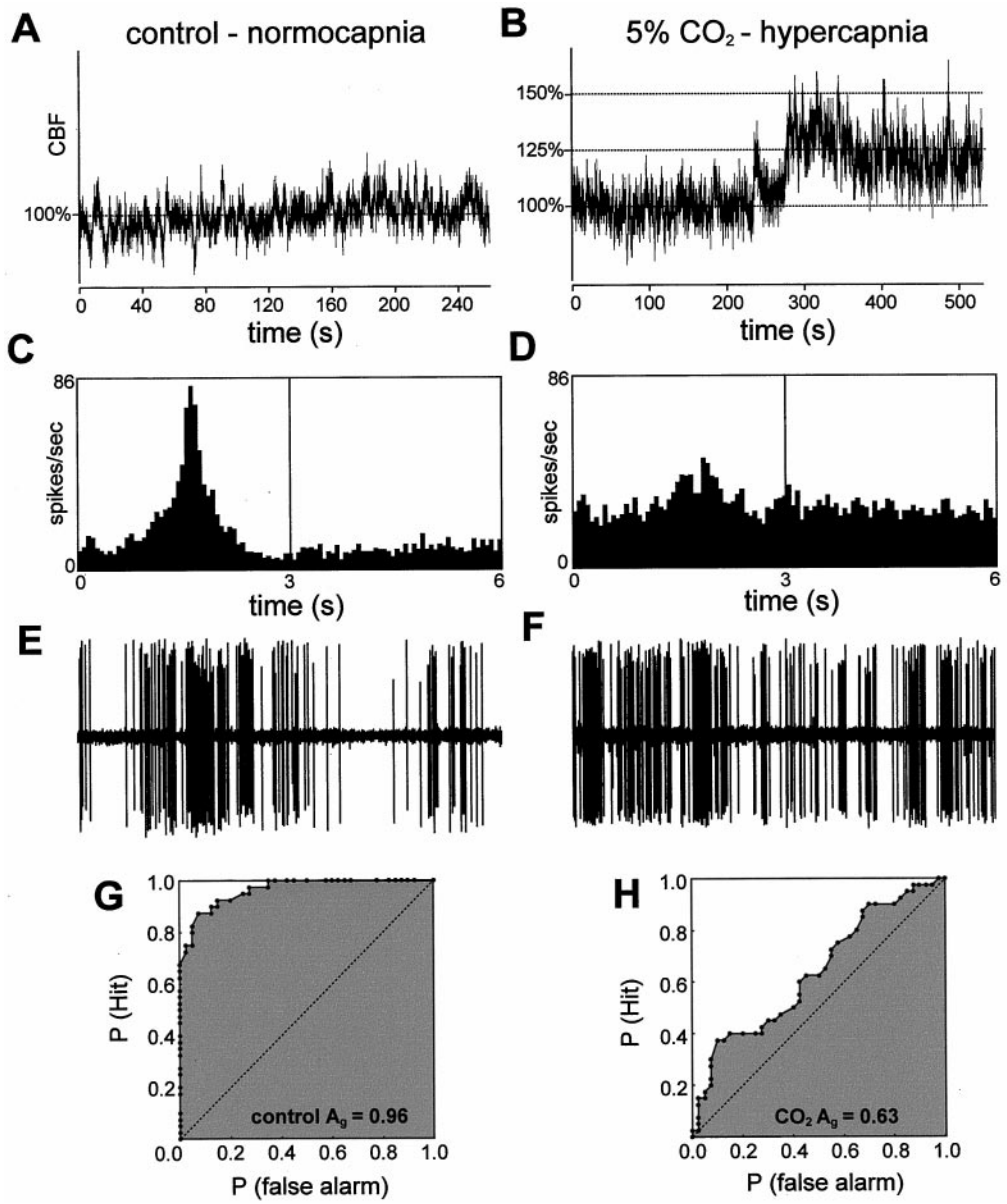

Figure 10. Effects of blood flow manipulation on neuronal signal detection. Blood flow and neuronal responses are shown for a single cell, recorded during control conditions and during 5% CO_2 inhalation. Relative changes of CBF as shown in *A* and *B* were measured with laser Doppler flowmetry from a probe placed on the surface of the visual cortex. Neuronal discharges for the two conditions are shown as PSTHs (*C, D*) and single trials of raw waveform of action potentials (*E, F*). In PSTHs, visual stimuli are presented from 0 to 3 sec, and idle time is presented at 3–6 sec. Increase in cortical blood flow by ~25% via 5% CO_2 inhalation decreased the detection capacity (as evaluated by the ROC metric) from 0.96 (*G*) to 0.63 (*H*).

of the range of neuronal actions of NO in the intact cerebral cortex. This interpretation is based on our observations that (1) opposing effects of NOS manipulation could be recorded simultaneously from neighboring neurons at the same recording sites or separately from neurons at different sites, and (2) differential effects can occur to ON versus OFF subfields of an individual neuron during NOS inhibition. Moreover, alternative methods for increasing cerebral blood flow (Fig. 10) do not mimic the effects of L-ARG on cell visual responses.

NO increases visual responses

When the population data from all cells are treated together, our results using trial-by-trial analysis show that, overall, NOS inhibitors (L-NA and L-MMA) significantly reduce visually evoked responses and that the natural NOS substrate (L-ARG) significantly facilitates evoked responses. In two earlier studies, comparisons of cumulative PSTHs in response to iontophoretic delivery of these same compounds in cortex found opposite effects on some tested cells, i.e., facilitatory actions of NOS inhibitors (Cudeiro et al., 1997) and inhibitory effects of L-ARG (Rivadulla et al., 1997). To address this discrepancy, we used quantitative trial-by-trial statistics on each cell to verify the fraction of cells that show significant inhibitory versus facilitatory effects on NOS manipulation.

In the visual cortex, Cudeiro et al. (1997) reported an incidence of effects with NOS inhibitor application in 38% of the tested cells and reported no facilitatory actions of L-ARG. Our quantitative analysis with spike-counting methods revealed that NOS inhibition significantly alters the visual response in most (83%) neurons

(see Fig. 3*C*). The lower incidence of effects reported by Cudeiro et al. (1997) may also be attributable to differences in anesthetic used. During electrophysiological recording, Cudeiro et al. (1997) used halothane, whereas we used a steroid (Saffan) administered intravenously. Interestingly, halothane inhalation anesthesia, but not intravenously applied anesthetics, has been shown to potently reduce neuronal NOS activity (Tobin et al., 1994) and the formation of cGMP from one of the primary targets of NO, guanylyl cyclase (Rengasamy et al., 1997). In our study of cortical neurons and in another study of thalamic neurons (Do et al., 1994), which used noninhalation anesthetics, the predominant effect of L-ARG administration is a marked enhancement of evoked activity. Rivadulla et al. (1997) reported long-lasting inhibitory effects of L-ARG in the visual cortex and argued that inhibitory effects of L-ARG were unrelated to the endogenous NO system, because these cells were unaffected by exogenous NO application and endogenous NOS blockade. We did not observe long-lasting inhibitory effects of L-ARG. The few cases of inhibitory effects recovered within 10 min of cessation of L-ARG iontophoresis. Facilitatory effects on visually evoked activity on direct exogenous application of an NO donor molecule (DEA-NO) suggest that the effects with L-ARG observed *in vivo* could be mediated through the endogenous NO pathway.

Because both L-ARG and L-LYS enter cells via the system y^+ carrier transport mechanism, which is Na^+-independent and electrogenically neutral (White, 1985), and because L-LYS had no effect on cells that had their response significantly modified by L-ARG, (Fig. 6*G*,*J*), then it is unlikely that an amino acid transport mechanism was responsible for L-ARG-mediated changes in visually evoked responses. Physiological stimulation of sensory afferents increases release of L-ARG (Do et al., 1994), presumably from glia (Aoki et al., 1991), and is therefore suggestive of a shuttling of L-ARG from glia to neurons via the extracellular space when neuronal activity increases. Furthermore, supplementation with exogenous L-ARG increases endogenous NO synthesis (Malinski et al., 1993) and facilitates neurotransmitter release *in vivo* (Strasser et al., 1994) and *in vitro* (Friedlander and Gancayco, 1996). Circulating levels of L-ARG (or other molecules) in the cerebrospinal fluid might have little bearing on its availability in the extracellular space (Montague, 1996; see Nicholson and Sykova, 1998). These findings suggest that L-ARG need not be rate-limiting *in vivo*.

Our recording methods allowed us to occasionally record from two well isolated neurons simultaneously while performing various pharmacological manipulations. The observation that opposing effects (with L-ARG or L-MMA iontophoresis) can be obtained in this circumstance argue against the possibility of opposite effects arising from the sequential order of different drug applications at different sites in a single electrode penetration. Together with lack of effects with D-forms of arginine analogs, recording opposite effects at the same recording site also suggests that the occasional inhibitory actions of NO on visually evoked activity are not attributable to nonspecific pH or iontophoresis current effects of administering these compounds.

NO increases signal detection and decreases the coefficient of variation of evoked discharges

We used ROC and CV_{cnt} analysis to evaluate whether NO changes the ability of cells to detect a stimulus and the variability of the responses over a series of trials. Despite increases or decreases in spontaneous activity, the net effect of cortical NO was to increase signal detection. The absence of spontaneous activity in 56 of 122 cells (Table 1, groups 1–5) contributed to a large number of cases with near-perfect signal detection. Although complex cells generally display higher levels of spontaneous activity than simple cells, the significant increase in signal detection with endogenous NO upregulation and a significant decrease in signal detection with endogenous NO downregulation was not dependent on the class of receptive field structure (simple vs complex).

Traditionally, ROC methods have been used in signal detection experiments in which "near"-threshold and/or above-threshold visual stimuli are presented to ask an ideal observer (e.g., a single neuron or an organism) to discriminate between two stimuli that have small differences in parameters such as orientation, contrast, or spatial frequency of the visual stimulus (Thomas, 1983; Bradley et al., 1987; Skottun et al., 1987). However, recent studies have successfully used ROC methods with presentations of identical suprathreshold visual stimuli to ask whether signal detection changes in different cell types (Wilson et al., 1988), in different intrinsic states of neuronal discharge (Guido et al., 1995), or in the availability of a specific class of cell surface receptors (Godwin et al., 1996). Our study also used suprathreshold visual stimuli. Near-threshold visual stimuli would not allow us to test for bidirectional effects, i.e., downregulation and upregulation of NO production. However, contrast–response functions under control and drug conditions would allow for near-threshold analysis. The effects of NO may be different near visual response threshold. Indeed, our preliminary analysis ($n = 7$; J. Smith and M. J. Friedlander, unpublished observations) suggests that L-ARG may have even greater effects on these responses and increase the slope of the contrast response function.

Whether manipulations that alter NO production change signal to noise was addressed by performing CV_{cnt} analysis. NOS blockade significantly increased CV_{cnt}, and L-ARG significantly decreased CV_{cnt}. The change in CV_{cnt} was negatively correlated with the change in ROC, suggesting that the greater the normalized variability, the less the capacity of the cortical neuron to distinguish signal from noise (Godwin et al., 1996). This inverse relationship between change in ROC and CV_{cnt} allowed us to infer that for neurons that already had perfect signal detection during control conditions, NO-mediated decreases in coefficient of variation also reflect increased fidelity of signal detectability. This is consistent with the fact that for Gaussian distributions, the ROC Ag is the same as percent correct in a two-alternative forced-choice test representing the separation of two distributions in units of SD (Cohn et al., 1975; Macmillan and Creelman, 1991).

The ability of NO downregulation (by NOS inhibition with L-MMA or L-NA) or NO upregulation (by L-ARG) to increase and decrease the coefficient of variation of the responses, respectively, is expected based on renewal statistics (see Materials and Methods). However, we asked whether the change in CV in response to NO manipulation was greater than expected from the effect on the mean response magnitude alone. The relationships between measured and expected CVs for each of the three conditions (control, L-ARG, and L-MMA/L-NA) were fitted by linear regression analysis (control: Poisson, $y = 0.74x + 15.62$; $r = 0.59$; L-ARG: Poisson, $y = 0.60x + 18.35$; $r = 0.59$; and L-MMA/L-NA: Poisson, $y = 0.94x + 13.84$; $r = 0.82$). The regression lines of the L-ARG Poisson versus the L-MMA/LNA Poisson data sets were significantly different ($p < 0.003$, t test), suggesting that the change in CV was greater than that predicted from the change in response magnitude alone. However, the L-ARG Poisson and

L-MMA/LNA Poisson distributions were not significantly different ($p = 0.17$ and $p = 0.07$, respectively) from the control Poisson distribution, although the direction of the changes in slope of the regression lines was consistent with an added contribution of NO to reducing variability. Thus, endogenous NO production contributes to cortical neuron responsiveness through several processes: enhanced signal detection, increased signal-to-noise ratio, and, to a lesser extent, decreased trial-by-trial response variability.

The observation that NO mediates enhancement of the visually evoked discharge is consistent with an NO- and L-ARG-mediated increase in L-glutamate release at active but not quiescent synapses (Friedlander and Gancayco, 1996). However, NO also can enhance the release of other neurotransmitters, such as GABA (Kano et al., 1998) and norepinephrine (Montague et al., 1994). Irrespective of the range of NO diffusion and whether NO is enhancing excitatory or inhibitory transmitter release, or a combination of both, our results suggest that the net effect of cortical NO is to increase signal detectability of neurons. How NO decreases the coefficient of variation of evoked discharges is uncertain. One possibility is that because NO increases glutamate release, the greater synaptic current drives the postsynaptic neuron to higher spike discharge rates. This could enhance the regularity of the discharge as the neuron approaches its maximal firing rate because of the refractory period of action potentials (Mainen and Sejnowski, 1995; Holt et al., 1996; Berry and Meister, 1998). Although the response might saturate over a brief period, discharge at the maximal rate need not be limiting, because neurons could fire even more spikes over a longer period. (Berry and Meister, 1998). We evaluated this possibility by comparing the interspike interval (ISI) distributions during the visual response under control versus upregulation of NO by L-ARG or DEA-NO iontophoresis. In the 29 cases in which L-ARG or DEA-NO facilitated the magnitude of the visual response, the mean ISI was reduced from 49.50 ± 8.59 (SEM) to 35.13 ± 4.64 (SEM) msec, whereas the fraction of ISIs approaching the refractory period (1–5 msec) increased from 18 to 22% of ISIs, with 25 of 29 cells showing a relative increase in these shortest ISIs during NO upregulation ($z = 2.65$; $n = 29$; $p < 0.05$, Wilcoxon signed-rank test).

Targets for NO-enhancing signal detection

Parsing the vascular versus direct neural effects of signaling molecules, including neurotransmitters (e.g., norepinephrine) *in vivo*, is difficult. For example, nonepinephrine decreases arteriole diameter but increases neuronal excitability, presumably through a decrease in O_2 supply (Stone, 1971). In the present study, it was found that NOS inhibition typically depressed the visual response. Topical applications of L-ARG (and presumed enhancement of NO production) produces an increase of pial arteriole diameter by only 6% in normotensive animals (Riedel et al., 1995). In addition, previously published *in vitro* slice and biochemical studies from visual cortical tissue demonstrate that NO has specific neuronal effects (Montague et al., 1994; Friedlander and Gancayco, 1996; Harsanyi and Friedlander, 1997a,b; for review, see Kara and Friedlander, 1998). Consequently, several lines of independent evidence provide support for direct neuronal effects of NO in the cerebral cortex, independent of influences from the vasculature. The implications of similar actions from our findings *in vivo* would be facilitated if perfect pharmacological separation of vascular from direct neuronal effects of NO *in vivo* could be achieved. 7-Nitro-indazole (7-Ni), a synthetic compound initially thought to be a selective inhibitor of nNOS (Moore et al., 1993) and thus absent of vascular effects, has recently been shown to significantly increase systemic arterial blood pressure (Zagvazdin et al., 1996), reduce eNOS activity (Fabricius et al., 1996), and relax vascular smooth muscle in an NO-independent manner (Medhurst et al., 1994). Consequently, 7-Ni was not used to attempt to dissociate whether the NO-mediated changes in visual responses were nNOS- or eNOS-dependent.

The other lines of evidence that we obtained *in vivo* that address the issue of the sites of NO action include the simultaneous dual recordings from neighboring neurons in response to iontophoretic manipulation of NO levels and the quantitative analysis of receptive field structure. Although, as described above, the statistically significant overall population effect of NO on the 122 cells tested was to enhance the visual responses of the cells (and increase signal detection in a subset of those cells), occasionally opposite effects occurred. Using this observation to advantage, we were able to record from 13 pairs of cells, of which three simultaneously recorded pairs had such opposing effects. The argument may be made that the lack of an effect on one of the neighboring cells may be attributable to that cell being out of range of the iontophoretic delivery of the L-ARG or L-NA/L-MMA or of the subsequent diffusion of NO. However, in the cell pairs in which opposing actions of L-ARG occurred, the smaller-amplitude spike (presumably indicative of the cell farthest from the electrode tip) could have its visual response facilitated or inhibited, and it was just as likely for the smaller spike to be affected, whereas the larger spike (presumably the nearer cell) was unaffected. Thus, the ability of NO to have these differential effects *in vivo* is more likely indicative of multiple neuronal target pathways (neurotransmitter release, NMDA receptors, and ion channels) of which a particular class of actions predominate at a given cell or synapse. Although these observations do not preclude the possibility of NO exerting neuronal actions indirectly via vasodilation, they are consistent with the known direct neural actions of NO. A similar argument can be made for our results on the NO effects on the ON–OFF substructure of the simple cell receptive fields. The occasional selective effects on one subfield of a cell are not readily reconciled with the predominant effect of NO on the visual responses of these neurons being a result of a general effect of enhanced blood flow. It is unlikely that the different synaptic inputs from the ON-center and OFF-center geniculocortical neurons that provide the subfields to a simple cortical neuron would be selectively modulated by blood flow changes. Moreover, the occasional examples of L-ARG reducing the magnitude of the subfields (see Fig. 9*B*) to stationary visual stimuli or the response to moving stimuli (see Fig. 8*C*) are also consistent with a direct neuronal action versus indirect vascular action, because increasing local blood flow (as would be expected from increasing NO production from L-ARG delivery) would be expected to uniformly affect responses.

The third line of evidence consistent with a direct neuronal action of endogenous cortical NO is derived from the blood flow measurement experiment. Our direct measures of cortical blood flow with a laser Doppler probe during microiontophoresis of the arginine compounds revealed no detectable changes, although neuronal responses were affected (data not shown). This result could be attributable to lack of a vascular effect or to such an effect being below the detection limits of the laser Doppler probe. However, in other experiments, more global and readily detectable increases in cerebral blood flow were induced with alternative methods, including hypercapnia via inspiration of 5% CO_2. In these cases, although the spontaneous activity of individual

neurons increased with increasing CBF, signal detection worsened (Fig. 10), opposite to the effects of L-ARG iontophoresis (Figs. 1*C*, 2*B*, 5*B,D,F,H*, 6*B,D,F,I*). These results are consistent with the differential dual recording (Fig. 8) and receptive field spatial profile (Fig. 9) results and the interpretation that the effects of NO on individual neuron visual responses induced by microiontophoresis of L-ARG or L-MMA are primarily attributable to direct neuronal effects versus indirect effects, secondary to changes in cortical blood flow. However, a contribution of CBF to the visual responses that may occur from the arginine iontophoresis procedures cannot be excluded, because the more global manipulation of CBF by hypercapnia could potentially have other effects on neighboring areas of cortex that could offset the local blood flow effects. When considered together, all of our results are consistent with a contribution from direct neuronal action of NO. Future experiments will require laser Doppler technology with much smaller microprobes to directly assess *in vivo* changes in microvascular perfusion in response to microiontophoretic administration of NO-modulating compounds coupled with electrophysiological recording from individual neurons at the same site.

Implications of cortical NO production for sensory signal processing

Considering that the visual world is filled with complex scenes, increasing signal detection of neurons might be an important adaptation to help the organism extract important cues from the environment. The data presented in this paper suggest that a simple molecule of two atoms (NO), serving as a diffusible messenger in a volume of cortical tissue, can facilitate the visual response magnitude of sensory neurons and their ability to detect signals. Many striate cortical cells act as near-perfect signal detectors (with optimally configured visual stimuli) under resting conditions with basal production of endogenous NO. In these cells, the predominant effect of NO is to increase the overall level of the visual response, although occasional suppressive effects occur. These different effects of NO might be attributable to the pharmacological substances accessing different sources of NO. At least four different potential sources of intracortical NO are present in the neocortex: from intrinsic intracortical neurons that can be excitatory or inhibitory (Aoki et al., 1997), subplate cells located below layer 6 in the white matter, which appear to be of both smooth and spiny varieties (Clancy et al., 1997), dorsal raphe serotonergic neurons (Friedlander et al., 1995), and from extrinsic cholinergic brainstem inputs (Bickford et al., 1993). The proximity of the NO-generating processes of these cells to particular synapses and varying levels of basal NO production between them could provide a substrate for differential effects on their neighboring cells and synapses. Our results suggest that endogenous NO plays a role in a form of dynamic modification of cortical neuron visual responses, although which intracortical cellular sources specifically contribute to the effects cannot be determined from our study. Neuronal and molecular mechanisms of increasing signal detection to extract salient features in the environment are likely to be important throughout development and in adulthood, as supported by our observation of similar effects of transient modifications in local NO production on visual responses in both kittens and adults. The local modulation of NO levels in defined visual cortical volumes may provide enhanced signal detection at appropriate spatiotemporal domains. For example, attentional shifts (Treue and Maunsell, 1996; Roelfsema et al., 1998) or changing the assemblage of functional neuronal ensembles (Singer, 1995; Logothetis, 1998) based on recent experience or stimulus relevance may require transient local changes in subsets of synaptic weights (Bienenstock et al., 1982). Understanding how such local control of NO levels is achieved requires additional information about the source of the synaptic inputs, the cortical innervation pattern, and the local regulation of dendritic and axonal NO production of the intrinsic calcium-activated NOS-containing neurons that innervate the visual cortex. Other features of striate cortical neurons that may play a role in feature extraction include the higher spatial and temporal resolution of bicellular receptive fields that are fully developed in the kitten visual cortex by 4 weeks of age (Freeman, 1996). The signal-enhancing property of NO is likely to be achieved by modulating the release of excitatory (and perhaps inhibitory) neurotransmitters at co-active synapses that are driven by salient visual stimuli. The current findings in cat striate cortex should be extended to other visual areas and experimental preparations in which there is a higher incidence of spontaneous activity in individual neurons allowing further characterization of the extent of NO in increasing signal detection in sensory signal processing in the cerebral cortex in general. In both striate and extrastriate regions, analysis of neuronal discharges before and during NO modulation using "noisy" visual stimuli presented as isodipole (Purpura et al., 1994), drifting (Casanova et al., 1995), and/or figure-ground textures (Zipser et al., 1996) might provide more direct evidence of the ability of NO to facilitate cortical neurons to extract salient features from complex visual scenes.

REFERENCES

Ahissar E, Vaadia E, Ahissar M, Bergman H, Arieli A, Abeles M (1992) Dependence of cortical plasticity on correlated activity of single neurons and on behavioral context. Science 257:1412–1414.

Aoki C, Fenstemaker S, Lubin M, Go C-G (1993) Nitric oxide synthase in the visual cortex of monocular monkeys as revealed by light and electron microscopic immunocytochemistry. Brain Res 620:97–113.

Aoki C, Rhee J, Lubin M, Dawson TM (1997) NMDA-R1 subunit of the cerebral cortex co-localizes with neuronal nitric oxide synthase at pre- and postsynaptic sites and in spines. Brain Res 750:25–40.

Aoki D, Semba R, Mikoshiba K, Kashiwamata S (1991) Predominant localization in glial cells of free L-arginine. Immunocytochemical evidence. Brain Res 547:190–192.

Arancio O, Kiebler M, Lee CJ, Lev-Ram V, Tsien RY, Kandel ER, Hawkins RD (1996) Nitric oxide acts directly in the presynaptic neuron to produce long-term potentiation in cultured hippocampal neurons. Cell 87:1025–1035.

Berry MJ, Meister M (1998) Refractoriness and neural precision. J Neurosci 18:2200–2211.

Bickford ME, Gunluk AE, Guido W, Sherman SM (1993) Evidence that cholinergic axons from the parabrachial region of the brainstem are the exclusive source of nitric oxide in the lateral geniculate nucleus of the cat. J Comp Neurol 334:410–430.

Bienenstock EL, Cooper LN, Munro PW (1982) Theory for the development of neuron selectivity: orientation specificity and binocular interaction in visual cortex. J Neurosci 2:32–48.

Bond A, Lodge D (1995) Pharmacology of metabotropic glutamate receptor-mediated enhancement of responses to excitatory and inhibitory amino acids on rat spinal neurons *in vivo*. Neuropharmacology 34:1015–1023.

Bradley A, Skottun BC, Ohzawa I, Sclar G, Freeman RD (1987) Visual orientation and spatial frequency discrimination: a comparison of single neurons and behavior. J Neurophysiol 57:755–772.

Budai D, Wilcox GL, Larson AA (1995) Effects of nitric oxide availability on responses of spinal wide dynamic range neurons to excitatory amino acids. Eur J Pharmacol 278:39–47.

Casanova C, Savard T, Nordmann JP, Molotchnikoff S, Minville K (1995) Comparison of the responses to moving texture patterns of simple and complex cells in the cat's area 17. J Neurophysiol 74:1271–1286.

Chung S, Ferster D (1998) Strength and orientation tuning of the thalamic input to simple cells revealed by electrically evoked cortical suppression. Neuron 20:1177–1189.

Clancy B, Da Silva Filhu M, Hester F, Friedlander MJ (1997) Structure, function, and connectivity of white matter neurons in mammalian visual cortex. Soc Neurosci Abstr 23:1268.

Cohn TE, Green DG, Tanner WP (1975) Receiver operating characteristic analysis: Analysis to the study of quantum fluctuation effects in optic nerve of *Rana pipiens*. J Gen Physiol 66:583–616.

Cormier RT, Mauk MD, Kelly PT (1993) Glutamate iontophoresis induces long-term potentiation in the absence of evoked presynaptic activity. Neuron 10:907–919.

Cressie NAC (1993) Statistics for spatial data. New York: Wiley.

Cruikshank SJ, Weinberger NM (1996) Receptive-field plasticity in the adult auditory cortex induced by hebbian covariance. J Neurosci 16:861–875.

Cudeiro J, Rivadulla C, Rodriguez R, Martinez-Conde S, Martinez L, Grieve KL, Acuna C (1996) Further observations on the role of NO in the feline lateral geniculate nucleus. Eur J Neurosci 8:144–152.

Cudeiro J, Rivadulla C, Rodriguez R, Grieve KL, Martinez-Conde S, Acuna C (1997) Actions of compounds manipulating the nitric oxide system in the cat primary visual cortex. J Physiol (Lond) 504:467–478.

de Ruyter van Steveninck RR, Lewen GD, Strong SP, Koberle R, Bialek W (1997) Reproducibility and variability in neural spike trains. Science 275:1805–1808.

Dinerman JL, Dawson TM, Schell MJ, Snowman A, Snyder SH (1994) Endothelial nitric oxide synthase localized to hippocampal pyramidal cells: Implications for synaptic plasticity. Proc Natl Acad Sci USA 91:4214–4218.

Do K-Q, Binns KE, Salt TE (1994) Release of the nitric oxide precursor, arginine, from the thalamus upon sensory afferent stimulation, and its effect on thalamic neurons *in vivo*. Neuroscience 60:581–586.

Fabricius M, Rubin I, Bundgaard M, Lauritzen M (1996) NOS activity in brain and endothelium: relation to hypercapnic rise of cerebral blood flow in rats. Am J Physiol 271:H2035–H2044.

Ferster D, Chung S, Wheat H (1996) Orientation selectivity of thalamic input to simple cells of cat visual cortex. Nature 380:249–252.

Freeman RD (1996) Studies of functional connectivity in the developing and mature visual cortex. J Physiol (Paris) 90:199–203.

Friedlander MJ, Gancayco C (1996) Selective enhancement of glutamate release by interaction of peroxynitrite and a voltage-gated calcium signal. Soc Neurosci Abstr 22:507.

Friedlander MJ, Hester FW, Gancayco CD, Waterhouse BD, Lin RCS (1995) The role of the ascending serotonergic system in cortical nitric oxide production. Soc Neurosci Abstr 21:1753.

Friedlander MJ, Harsanyi K, Dudek S, Kara P (1996) Developmental mechanisms for regulating signal amplification at excitatory synapses in the neocortex. In: Neural development and plasticity (Mize RR, Erzurumlu RS, eds). Prog Brain Res 108:245–262. Amsterdam: Elsevier.

Garthwaite J, Boulton CL (1995) Nitric oxide signaling in the central nervous system. Annu Rev Physiol 57:683–706.

Godwin DW, Vaughan JW, Sherman SM (1996) Metabotropic glutamate receptors switch visual response mode of lateral geniculate nucleus cells from burst to tonic. J Neurophysiol 76:1800–1816.

Guido W, Lu S-M, Vaughan JW, Godwin DW, Sherman SM (1995) Receiver operating characteristic (ROC) analysis of neurons in the cat's lateral geniculate nucleus during tonic and burst response mode. Vis Neurosci 12:723–741.

Harsanyi K, Friedlander MJ (1997a) Transient synaptic potentiation in the visual cortex. I. Cellular mechanisms. J Neurophysiol 77:1269–1283.

Harsanyi K, Friedlander MJ (1997b) Transient synaptic potentiation in the visual cortex. II. Developmental regulation. J Neurophysiol 77:1284–1295.

Holt GR, Softky WR, Koch C, Douglas RJ (1996) Comparison of discharge variability *in vitro* and *in vivo* in cat visual cortex neurons. J Neurophysiol 75:1806–1814.

Hosokawa H, Sawamura T, Kobayashi S, Ninomiya H, Miwa S, Masaki T (1997) Cloning and characterization of a brain-specific cationic amino acid transporter. J Biol Chem 272:8717–8722.

Huang PL, Dawson TM, Bredt DS, Snyder SH, Fishman MC (1993) Targeted disruption of the neuronal nitric oxide synthase gene. Cell 75:1273–1286.

Irikura K, Huang PL, Ma J, Lee WS, Dalkara T, Fishman MC, Dawson TM, Snyder SH, Moskowitz MA (1995) Cerebrovascular alterations in mice lacking neuronal nitric oxide synthase gene expression. Proc Natl Acad Sci USA 92:6823–6827.

Kano T, Shimizu F, Huang P, Moskowitz M, Lo E (1998) Effect of nitric oxide synthase gene knockout on neurotransmitter release *in vivo*. Neuroscience 86:695–699.

Kara P, Friedlander MJ (1998) Dynamic modulation of cerebral cortex synaptic function by nitric oxide. In: Nitric oxide in brain development, plasticity, and disease (Mize RR, Dawson TM, Dawson VL, Friedlander MJ, eds). Prog Brain Res 118:183–198. Amsterdam: Elsevier.

Kavanaugh MP (1993) Voltage dependence of facilitated arginine flux mediated by the system y+ basic amino acid transporter. Biochemistry 32:5781–5785.

Levine ES, Jacobs BL (1992) Neurochemical afferents controlling the activity of serotonergic neurons in the dorsal raphe nucleus: microiontophoretic studies in the awake cat. J Neurosci 12:4037–4044.

Lev-Ram V, Jiang T, Wood J, Lawrence DS, Tsien RY (1997) Synergies and coincidence requirements between NO, cGMP, and Ca2+ in the induction of cerebellar long-term depression. Neuron 18:1025–1038.

Logothetis N (1998) Object vision and visual awareness. Curr Opin Neurobiol 8:536–544.

Macmillan NA, Creelman CD (1991) Detection theory: a user's guide. New York: Cambridge UP.

Mainen ZF, Sejnowski TJ (1995) Reliability of spike timing in neocortical neurons. Science 268:1503–1506.

Malen PL, Chapman PF (1997) Nitric oxide facilitates long-term potentiation, but not long-term depression. J Neurosci 17:2645–2651.

Malinski T, Radomski MW, Taha Z, Moncada S (1993) Direct electrochemical measurement of nitric oxide released from human platelets. Biochem Biophys Res Commun 194:960–965.

Markram H, Tsodyks M (1996) Redistribution of synaptic efficacy between neocortical pyramidal neurons. Nature 382:807–810.

Marletta MA (1994) Nitric oxide synthase: aspects concerning structure and catalysis. Cell 78:927–930.

Medhurst AD, Greenlees C, Parsons AA, Smith SJ (1994) Nitric oxide synthase inhibitors 7- and 6- nitroindazole relax smooth muscle *in vitro*. Eur J Pharmacol 256:R5–R6.

Merrill EG, Ainsworth A (1972) Glass-coated platinum-plated tungsten microelectrodes. Med Biol Eng 10:662–671.

Moncada S (1997) Nitric oxide in the vasculature: physiology and pathophysiology. Ann NY Acad Sci 811:60–67.

Moncada S, Palmer RMJ, Higgs EA (1991) Nitric oxide: physiology, pathophysiology, and pharmacology. Pharmacol Rev 43:109–142.

Montague PR (1996) The resource consumption principle: attention and memory in volumes of neural tissue. Proc Natl Acad Sci USA 93:3619–3623.

Montague PR, Gancayco CD, Winn MJ, Marchase RB, Friedlander MJ (1994) Role of NO production in NMDA receptor-mediated neurotransmitter release in cerebral cortex. Science 263:973–977.

Moore PK, Babbedge RC, Wallace P, Gaffen ZA, Hart SL (1993) 7-Nitro indazole, an inhibitor of nitric oxide synthase, exhibits antinociceptive activity in the mouse without increasing blood pressure. Br J Pharmacol 108:296–297.

Nathan C, Xie Q-W (1994) Nitric oxide synthases: Rolls, tolls, and controls. Cell 78:915–918.

Nicholson C, Sykova E (1998) Extracellular space structure revealed by diffusion analysis. Trends Neurosci 21:207–215.

Obeid AN, Barnett NJ, Dougherty G, Ward G (1990) A critical review of laser Doppler flowmetry. J Med Eng Technol 14:178–181.

Ohkuma S, Katsura M, Guo J-L, Hasegawa T, Kuriyama K (1995) Involvement of peroxynitrite in *N*-methyl-D-asparate- and sodium nitroprusside-induced release of acetylcholine from mouse cerebral cortical neurons. Mol Brain Res 31:185–193.

Ohkuma S, Katsura M, Chen D-Z, Narihara H, Kuriyama K (1996) Nitric oxide-evoked [^{3}H]γ-aminobutyric acid release is mediated by two distinct release mechanisms. Mol Brain Res 36:137–144.

Pettigrew JD, Cooper ML, Blasdel GG (1979) Improved use of tapetal reflection for eye-position monitoring. Invest Ophthalmol Vis Sci 18:490–495.

Pirot S, Godbout R, Mantz J, Tassin JP, Glowinski J, Thierry AM (1992) Inhibitory effects of ventral tegmental area stimulation on the activity of prefrontal cortical neurons: evidence for the involvement of both dopaminergic and GABAergic components. Neuroscience 49:857–865.

Purpura KP, Victor JD, Katz E (1994) Striate cortex extracts higher-order spatial correlations from visual textures. Proc Natl Acad Sci USA 91:8482–8486.

Recanzone GH, Schreiner CE, Merzenich MM (1993) Plasticity in the

frequency representation of primary auditory cortex following discrimination training in adult owl monkeys. J Neurosci 13:87–103.
Reid RC, Alonso JM (1995) Specificity of monosynaptic connections from thalamus to visual cortex. Nature 378:281–284.
Reid SNM, Daw NW, Czepita D, Flavin HJ, Sessa WC (1996) Inhibition of nitric oxide synthase does not alter ocular dominance shifts in kitten visual cortex. J Physiol (Lond) 492:511–517.
Rengasamy A, Pajewski TN, Johns RA (1997) Inhalation anesthetic effects on rat cerebellar nitric oxide and cyclic guanosine monophosphate production. Anesthesiology 86:689–698.
Riedel MW, Anneser F, Harberl RL (1995) Different mechanisms of L-arginine induced dilation of brain arterioles in normotensive and hypertensive rats. Brain Res 671:21–26.
Rivadulla C, Grieve KL, Rodriguez R, Martinez-Conde S, Acuna C, Cudeiro J (1997) An unusual effect of application of the amino acid L-arginine on the cat visual cortical cells. NeuroReport 8:863–866.
Roelfsema PR, Lamme VA, Spekreijse H (1998) Object based attention in the primary visual cortex of the macaque monkey. Nature 395:376–381.
Ruthazer ES, Gillespie DC, Dawson TM, Snyder SH, Stryker MP (1996) Inhibition of nitric oxide synthase does not prevent ocular dominance plasticity in kitten visual cortex. J Physiol (Lond) 492:519–527.
Schuman EM, Madison DV (1991) A requirement for the intercellular messenger nitric oxide in long-term potentiation. Science 254:1503–1506.
Schuman EM, Madison DV (1994) Locally distributed synaptic potentiation in the hippocampus. Science 263:532–536.
Shadlen MN, Newsome WT (1998) The variable discharge of cortical neurons: implications for connectivity, computation, and information coding. J Neurosci 18:3870–3896.
Shibuki K, Okada D (1991) Endogenous nitric oxide release required for long-term synaptic depression in the cerebellum. Nature 349: 326–328.
Singer W (1995) Development and plasticity of cortical processing architectures. Science 270:758–764.
Skottun BC, Bradley A, Sclar G, Ohzawa I, Freeman RD (1987) The effects of contrast on visual orientation and spatial frequency discrimination: a comparison of single cells and behavior. J Neurophysiol 57:773–786.
Snyder SH (1992) Nitric oxide: first in a new class of neurotransmitters. Science 257:494–496.
Sokal RR, Rohlf FJ (1995) Biometry. New York: Freeman.
Son H, Hawkins RD, Martin K, Kiebler M, Huang PL, Fishman MC, Kandel ER (1996) Long-term potentiation is reduced in mice that are doubly mutant in endothelial and neuronal nitric oxide synthase. Cell 87:1015–1023.
Song H, Ming G, Fon E, Bellocchio E, Edwards RH, Poo M (1997) Expression of a putative vesicular acetylcholic transpsorter facilitates quantal transmitter packing. Neuron 18:815–826.
Stone TW (1971) Are noradrenaline excitations artefacts? Nature 234:145–146.
Stone TW (1985) Microiontophoresis and pressure ejection. New York: Wiley.
Strasser A, McCarron RM, Ishii H, Stanimirovic D, Spatz M (1994) L-Arginine induces dopamine release from the striatum *in vivo*. NeuroReport 5:2298–2300.
Thomas JP (1983) Underlying psychometric function for detecting gratings and identifying spatial frequency. J Opt Soc Am 73:751–758.
Tobin JR, Martin LD, Breslow MJ, Traystman RJ (1994) Selective anesthetic inhibition of brain nitric oxide synthase. Anesthesiology 81:1264–1269.
Treue S, Maunsell JH (1996) Attentional modulation of visual motion processing in cortical areas MT and MST. Nature 382:539–541.
White MF (1985) The transport of cationic amino acids across the plasma membrane of mammalian cells. Biochim Biophys Acta 822:355–374.
Williams GV, Goldman-Rakic PS (1995) Modulation of memory fields by dopamine D1 receptors in prefrontal cortex. Nature 376:572–575.
Wilson JR, Bullier J, Norton TT (1988) Signal-to-noise comparisons for X and Y cells in the retina and lateral geniculate nucleus of the cat. Exp Brain Res 70:399–405.
Zagvazdin Y, Sancesario G, Wang Y-X, Share L, Fitzgerald MEC, Reiner A (1996) Evidence from its cardiovascular effects that 7-nitroindazole may inhibit endothelial nitric oxide synthase *in vivo*. Eur J Pharmacol 303:61–69.
Zipser K, Lamme VAF, Schiller PH (1996) Contextual modulation in primary visual cortex. J Neurosci 16:7376–7389.